Simulating functional diversity of European natural forests along climatic gradients

1
2
3

to be submitted to Journal of Biogeography

Running title: Functional diversity of European forests

Authors: Kirsten Thonicke[1,], Maik Billing[1,2,*], Werner von Bloh[1], Boris Sakschewski[1], Ülo Niinemets[3], Josep Peñuelas[4], Hans Cornelissen[5], Yusuke Onoda[6], Peter van Bodegom[7], Michael Schaepman[8], Fabian Schneider[9], Ariane Walz[2]*

[1] Research Domain 1 "Earth System Analysis", Potsdam Institute for Climate Impact Research (PIK), Member of the Leibniz Association, P.O. Box 60 12 03, D-14412 Potsdam, Germany

[2] Institute of Environmental Science and Geography, University of Potsdam, Karl-Liebknecht-Str. 24-25, 14476 Potsdam-Golm, Germany

[3] Estonian University of Life Sciences, Kreutzwaldi 1, 51006 Tartu, Estonia

[4] Global Ecology Unit CREAF-CSIC-UAB, Center for Ecological Research and Forestry Applications (CREAF) - National Research Council (CSIC) Edifici C, Universitat Autonoma de Barcelona, 08193 Bellaterra

[5] Systems Ecology, Department of Ecological Science, Vrije Universiteit, De Boelelaan 1085, 1081 HV Amsterdam, the Netherlands

[6] Division of Environmental Science and Technology, Graduate School of Agriculture, Kyoto University, Oiwake, Kitashirakawa, Kyoto, 606-8502, Japan

[7] Institute of Environmental Sciences, Department Environmental Biology, Leiden University, Einsteinweg 2, 2333 CC Leiden

[8] Remote Sensing Laboratories, Dept. of Geography, University of Zurich, Winterthurerstrasse 190, CH–8057 Zurich, Switzerland

[9] Jet Propulsion Laboratory, California Institute of Technology, 4800 Oak Grove Drive, Pasadena, CA 91011, USA

* Kirsten Thonicke and Maik Billing should be considered joint first author

Abstract

Aim

We analyse how functional diversity varies across European natural forests to understand the effects of environmental and competitive filtering on plant trait distribution.

Location

Forest ecosystems in Europe from 11°W to 36°E and 29.5°N to 62°N.

Taxon

Pinaceae, Fagaceae and Betulaceae, Oleaceae, Tiliaceae, Aceraceae, Leguminosae (unspecific).

Methods

We adopted the existing Dynamic Global Vegetation Model Lund-Potsdam-Jena managed Land of flexible individual traits (LPJmL-FIT) for Europe by eliminating both bioclimatic limits of plant functional types (PFTs) and replacing prescribed values of functional traits for PFTs with emergent values under influence of environmental filtering and competition. We quantified functional richness (FR), functional divergence (FDv) and functional evenness (FE) in representative selected sites and at Pan-European scale resulting from simulated functional and structural trait combinations of individual trees. While FR quantifies the amount of occupied trait space, FDv and FE describe the distribution and abundance of trait combinations, respectively, in a multidimensional trait space.

Results

LPJmL-FIT reproduces spatial PFTs and local trait distributions and agrees well with observed productivity, biomass and tree height of European natural forests. The observed site-specific trait distributions and spatial gradients of traits of the leaf- and stem-resource economics spectra coincide with environmental filtering and the competition for light and water in environments with strong abiotic stress. Where deciduous and needle-leaved trees co-occur, e.g. in boreal and mountainous forests, the potential niche space is wide (high FR), and extreme ends in the niche space are occupied (high FDv). We find high FDv in Mediterranean forests where drought increasingly limits tree growth, thus niche differentiation becomes more important. FDv decreases in temperate forests where a cold climate increasingly limits growth efficiency of broadleaved summergreen trees, thus reducing the importance of competitive exclusion. Highest FE was simulated in wet Atlantic and southern Europe which indicated relatively even niche occupation and thus high resource-use efficiency.

Main conclusions

We find functional diversity resulting from both environmental and competitive filtering. Pan-European FR, FDv and FE demonstrate the influence of climate gradients and intra- and inter-PFT competition. The indices underline a generally high functional diversity of natural forests in Europe. Co-existence of functionally diverse trees across PFTs emerges from alternative (life-history) strategies, disturbance and tree demography.

1. INTRODUCTION

Functional diversity (FD) is a key control of the stability and adaptability of ecosystems under climate change (Yachi and Loreau, 1999). Abiotic conditions (e.g. climate, soil) as well as biotic processes (e.g. competition) determine plant community assembly (Kunstler *et al.*, 2016; Ratcliffe *et al.*, 2017; Ruiz-Benito *et al.*, 2017), and thus the functional diversity of communities (Lavorel & Garnier, 2002a; Cadotte *et al.*, 2011; Naeem *et al.*, 2012). Ecosystem FD has been measured based on the diversity of morphological and/or physiological plant traits (Villeger *et al.*, 2008), which are linked to plant productivity, transpiration or nutrient cycling, and thus to ecosystem functions (cf. Lavorel & Garnier, 2002b). For instance, specific leaf area (SLA) and leaf nitrogen content have been linked to plant productivity, and stem traits such as wood density (WD) to carbon storage and evapotranspiration (Funk *et al.*, 2017) and, among others, determine species tolerance of environmental stresses (Hallik *et al.*, 2009) and control competitive interactions between individual plants (Kunstler *et al.*, 2016).

Under given climate conditions, the distribution of multiple individual traits results from community assembly rules and opens a multi-dimensional trait space of functionally related traits (Wright *et al.*, 2004; Mason *et al.*, 2005; Chave *et al.*, 2009; Díaz *et al.*, 2016). To quantify how environmental and competitive filtering influence niche complementarity, multidimensional indices of functional diversity are required to quantify occupation and overlap of niches (Mason & de Bello, 2013). In addition, these indices should be scale-independent and applicable at regional scale to investigate changes in FD along climatic gradients (Carmona *et al.*, 2016).

Climatic conditions are the most important drivers of community assembly and generally constrain the relations between traits globally (Butler *et al.*, 2017; Šímová *et al.*, 2018). Strong gradients in trait expression, associated to climatic conditions, have been found at global scales (Díaz *et al.*, 2016; Wright *et al.*, 2017) and at the European scale by extrapolating site-specific plant trait-data (Butler et al. 2017) and using forest inventories (Ruiz-Benito et al. 2017). Recent studies investigate a mix of globally important physiological traits (e.g., SLA, WD, seed mass and leaf nitrogen content) and morphological traits (including maximum plant height and basal area) (Ratcliffe *et al.*, 2016; Ruiz-Benito *et al.*, 2017), or separate the effects between those trait types (e.g. Madrigal-Gonzalez *et al.*, 2016; Schneider *et al.*, 2017). They advance our understanding of spatial pattern of plant traits at the landscape and continental scale.

Many different indices have been used to describe the size of trait spaces, the distribution and the clustering of their trait combinations (e.g. Ratcliffe *et al.*, 2016; Schneider *et al.*, 2017). Villéger et al. (2008) suggested to describe these FD aspects using three independent indices: functional richness (FR), divergence (FDv) and evenness (FE). While FR quantifies the amount of occupied trait space, FDv and FE describe the distribution and abundance of trait combinations in a multidimensional trait space (Mason *et al.*, 2005; Villeger *et al.*, 2008). While FR describes the size of potentially available, functional space, in which niches can be occupied by plants, FDv quantifies the distribution of trait values, thus

3

the degree of niche differentiation, likely the result from competitive exclusion (Mason *et al.*, 2005; Garnier *et al.*, 2016). FE describes the regularity of trait distribution and points to resource-use efficiency within the occupied trait space. Lower FR could relate to lower capability of an ecosystem to buffer environmental stress, whereas lower FE and FDv could indicate reduced ecosystem resilience (Mason *et al.*, 2005).

By dividing functional diversity into richness, divergence and evenness, the mechanisms that link biodiversity to ecosystem function and describe community assembly can be described (Mason *et al.*, 2005; Mason *et al.*, 2013). Computing scale-independent FD indices from trait distributions (Carmona *et al.*, 2016) allows investigating FD from community to meta-community scale and extrapolating them to the regional or continental scale. Huge efforts are under way to explore links between plant traits, vegetation composition and climate based on site data (Díaz *et al.*, 2016; Wright *et al.*, 2017; Bruelheide *et al.*, 2018). They are complemented by dynamic global vegetation models (DGVM) with flexible or adaptive individual traits (e.g., Sakschewski *et al.*, 2015; Langan *et al.*, 2017) which explore and map the mechanisms between functional diversity and ecosystem function from local to regional scales. The interplay between flexible morphological and physiological traits within plant functional types (PFT, Lavorel *et al.*, 2007; Prentice *et al.*, 2007) in combination with the physiology and biogeochemistry of a DGVM allows analysing the effect of community assembly on ecosystem function, e.g. productivity and carbon storage, in forest ecosystems. Because these flexible-trait DGVMs vary plant traits for individual trees that belong to a specific PFT, inter-PFT as well as the intra-PFT trait diversity are captured which allows investigating effects of niche complementarity along climatic gradients.

The overall aim of this study is to investigate the interaction between climate, ecosystem function and pattern of FD of forest ecosystems. We focus on European natural forests ranging from broadleaved evergreen vegetation in the Mediterranean basin, to temperate forests and to boreal forests in northern Europe. Here, natural forests are defined as potential natural forests whose compositions and ecosystem functions (see Mitchell, 2002; Hooper *et al.*, 2005; Geller *et al.*, 2017 for definition) results from climate and soil conditions. Forests and other wooded land are usually defined following the percentage of woody cover (FAO, 2018). However, we denote forests hereafter as vegetation with a significant amount of biomass (>50 gC/m²), at least 5% coverage of woody PFTs and a minimum mean tree height of 2m. For this study we adapted the DGVM LPJmL-FIT to PFTs growing in strongly seasonal European climatic conditions, while the model previously has been successfully applied to tropical rainforests (Sakschewski *et al.*, 2015). We break down the overall aim of the study into the following research questions:

1. What is the role of environmental and competitive filtering on trait distributions and productivity of Mediterranean, temperate and boreal natural forests?
2. How does functional diversity emerge from climate and plant competition at the local and pan-European scale?
3. How does functional diversity vary between and across European natural forests?

In order to address these research questions, we check the validity of the adapted LPJmL-FIT model by assessing to what degree the model reconstructs observed (a) productivity and

153   biomass, (b) trait distribution and (c) distribution of PFTs as a result of environmental and
154   competitive filtering. We quantify for selected sites and on a Pan-European scale FR, FDv
155   and FE of simulated physiological and morphological traits (cf. Villeger *et al.*, 2008;
156   Schneider *et al.*, 2017). We expect functional diversity to be generally high in natural forests
157   and climatic stressors considered in LPJmL-FIT to be a strong environmental filter.

158   Our analysis of functional diversity in natural forests can provide a reference state for
159   restoring highly managed or degraded ecosystems and increase their diversity and stability
160   in face of climate change (Liang *et al.*, 2016; Mori *et al.*, 2017). We focus here on the
161   interaction of physiological and morphological plant traits with community assembly
162   processes at the local and Pan-European scale to understand how functional diversity
163   emerges from those interactions.

164   2. MATERIALS AND METHODS

165   We connect the leaf and stem economics approach as implemented in LPJmL-FIT
166   (Sakschewski *et al.*, 2015) with a phenology model (Forkel et al. (2014) to simulate potential
167   natural vegetation in Europe under current climatic conditions. Herbaceous PFTs (C_3 and C_4
168   grasses) are simulated as in LPJmL (Schaphoff *et al.*, 2018b). To allow for environmental
169   and competitive filtering to take full effect within and across PFTs, we removed the
170   bioclimatic limits that are used in most DGVMs to emulate biogeographic limitations of PFT
171   occurrence (Sitch *et al.*, 2008; Schaphoff *et al.*, 2018b). Phenology, leaf-economics (LES)
172   and stem-economics (SES) traits (cf. Wright *et al.*, 2004; Chave *et al.*, 2009) are assigned to
173   each individual tree sapling at establishment allowing any trait combination (everything-is-
174   everywhere-approach, see Fig. 1 for trait-selection algorithm) whose competitiveness in a
175   given climate then determines its survival and growth. Physiology, growth and mortality of
176   trees within the forest patch are as described in Sakschewski *et al.* (2015). Applying this
177   simulation framework to current European climate, environmental and competitive filtering
178   result in site-specific trait distributions, productivity, biomass and in tree height.

179   2.1 Adjusted LPJmL-FIT model

180   LPJmL-FIT combines flexible individual traits with gap dynamics and plant physiology,
181   hydrology and biogeochemistry. Being structured into vertical leaf layers every two meters,
182   trees compete for light and water as they grow in size. The trait combination of each tree
183   determines its competitive strength under given climate conditions at a given site, where
184   several plant strategies can co-exist and form diverse communities in forest ecosystems.
185   The competitive interactions between individual trees through the suitability of their trait
186   combinations to the given climate, spatial distribution of traits change along respective
187   climatic gradients (Sakschewski *et al.*, 2015). In general, the model approach of LPJmL-FIT
188   allows all tree strategies to establish everywhere at any time ("everything is everywhere").
189   However, in equilibrium only those trees survive that are best adapted to the local
190   environmental conditions (climate and soil).

191 LPJmL-FIT was originally developed for Amazonian rainforests (Sakschewski *et al.*, 2015).
192 Adapting it to climatic conditions which are strongly seasonal and with a high intra-annual
193 variability requires a number of adaptations and implementations for multiple, co-occurring
194 PFTs to describe Mediterranean, temperate and boreal natural forests in Europe. The LES
195 and SES approach, as implemented in LPJmL-FIT, has therefore been adapted to
196 accommodate four tree PFTs, namely "broad-leaved summergreen" (BL-S), "broad-leaved
197 evergreen" (BL-E), "temperate needle-leaved" (T-NL) and "boreal needle-leaved trees" (B-
198 NL). Each PFT is based on an earlier implementation of these PFTs in LPJmL-4 (Schaphoff
199 *et al.*, 2018b) which has been extensively evaluated (Schaphoff *et al.*, 2018a). To account
200 for the phenology of the Mediterranean, temperate and boreal forests under the influence of
201 light, water and temperature stress, we implemented the phenology model of Forkel et al.
202 (2014) into LPJmL-FIT. This model couples the phenological status of a tree, which ranges
203 between zero (complete senescence) and one (fully leafed), to the local climate. The actual
204 value of the phenology status is determined by the product of four phenology functions,
205 which depend on a set of PFT-specific parameters and the daily temperature, water stress
206 and radiation. We calibrated the phenology parameter (Table S1) to yield a best possible
207 PFT distribution that matches the spatial distribution of European natural vegetation from
208 Bohn et. al (2007). Additionally, leaf senescence now occurs immediately if the phenological
209 status of a tree drops below 0.2, forcing a tree to rebuild the complete canopy leaf area in
210 the next simulation year. Given the climate influence on leaf phenology, BL-S trees imply a
211 continuous spectrum to winter-deciduous trees.

212 The algorithm to combine the PFT parameter set of the LES and SES-related traits with the
213 phenology parameter is implemented as follows: When a new sapling is established, the
214 selection of the trait combination occurs in three steps. First, the PFT type is randomly
215 chosen out of the four possible PFT independent of its climate suitability or the present PFT
216 composition (Fig. 1). Second, the selected PFT type defines the set of phenology
217 parameters that are assigned to the tree sapling (see Suppl. Table S1), and it defines the
218 SLA range from which the SLA value is drawn from a uniform distribution. The SLA range
219 differs for BL-E, T-NL, B-NL and BL-S (see Table S2). The functionally related plant traits
220 leaf longevity (LL), leaf N and Vcmax (maximum carboxylation rate of Rubisco per leaf area)
221 are assigned in a third step to the sapling following the LES approach as in Sakschewski *et*
222 *al.* (2015), see Fig. 1. Both, SLA and WD are drawn from a continuous uniform distribution
223 for each individual tree for which the PFT-specific range is derived from the TRY v4.0
224 database (see https://www.try-db.org/ Kattge *et al.*, 2011) considering only sites located
225 inside our study area. Hence, the parameter set of each newly established sapling in the
226 forest patch contains trait values drawn from the LES and SES as well as the phenology
227 parameters. Grasses are integrated in the model as homogeneous layers using the
228 remaining radiation at the bottom of every forest patch for photosynthesis. C_3 and C_4 grasses
229 compete with trees for water only. The establishment rate of grass is anti-proportional to the
230 actual tree cover and the mortality rate depends on carbon balance by the end of every year
231 (see Schaphoff et al. 2018 for details). Grasses are assigned phenology parameters (see
232 Table S1), but are simulated without individual trait flexibility following the LPJmL4 modelling

233   approach (Schaphoff *et al.*, 2018b). Therefore, in this study model simulations will be used to
234   evaluate trait distributions and functional diversity regarding trees only.

235   Different to the LPJmL-FIT version of Sakschewski *et al.* (2015), the trade-off between SLA
236   and LL has been adopted from LPJmL4 (Schaphoff *et al.*, 2018b):

237
$$LL = 10^{\frac{\beta_0 - \log_{10}\left(\frac{SLA}{\propto} \cdot DM_c\right)}{\beta_1}}$$
    (1)

238   where DM_c denotes the dry matter carbon content of leaves ($DM_c = 0.4763$) and the
239   parameter $\propto = 2 \cdot 10^{-4}$. The parameter β_1 is set to 0.4 and β_0 to 2.2 for broadleaved PFTs,
240   while $\beta_0 = 2.08$ for both, T-NL and B-NL. All parameters in equation (1) were obtained from
241   Kattge et al. (2011). The parameters β_1 and $\propto$ influence the steepness of the SLA-LL
242   relation, whereas β_1 alters the offset.

243   The mortality *mort_WD* is coupled to its wood density *WD* by using the equation from King et
244   al. (2006):

245
$$mort_{WD} = 10^{\alpha_1 + \alpha_2/WD}$$
    (2)

246   and assigned to each tree individual at establishment (Sakschewski *et al.*, 2015). Because
247   no general mortality-WD relationship for tree species of temperate forests is currently
248   available in the literature, we calibrated α_1 and α_2 to the locally observed biomass.
249   Calibration was carried out at European sites still containing natural forests (Hainich National
250   Park (NP) and Bialowieza NP), because the model simulates natural vegetation only.
251   Following this calibration, we set the parameter α_1 to -4.5 and α_2 to -2.66 for the broadleaved
252   trees, and $\alpha_1 = -2.66$ and $\alpha_2 = 0.255$ for needle-leaved trees. The term *mort_WD* is used as
253   the maximum of the growth-efficiency mortality in LPJmL-FIT, meaning that trees with a low
254   growth efficiency resulting from low productivity under unfavourable climate conditions have
255   a higher mortality risk (Sakschewski *et al.*, 2015).

256   Additionally, we reduced the tree allometry parameter *k_ep* to 1.5 (1.6 in Schaphoff *et al.*,
257   2018b) for needle-leaved trees to simulate realistic tree shapes and growth pattern of
258   needle- in comparison to broadleaved saplings:

259
$$CA \sim D^{k_{ep}}$$
    (3)

260   where *k_ep* mediates between crown area (CA) and stem diameter (D). The lower *k_ep*, the *CA*
261   for needle-leaved trees is reduced which then affects LAI:

262
$$LAI = \frac{C_{leaf} \cdot SLA}{CA}$$
    (4),

263   where C_{leaf} is whole plant carbon investment in leaves (kg per tree) (cf. Sitch *et al.*, 2003).
264   Because of the lower SLA, needle-leaved trees then have to invest more leaf carbon in their
265   first years to reach the same LAI compared to broadleaved trees.

266   Fire is an important natural disturbance in European forest ecosystems (Naveh, 1990;
267   Tinner, 1999). We applied the simple Glob-FIRM model (Thonicke *et al.*, 2001) as
268   embedded in LPJmL4. Here, fire probability depends on soil moisture in the top soil layer

269 and a fuel load threshold modelled by an exponential probability function calculated by the
270 end of every year. We apply this probability to each patch separately. If a patch is burnt,
271 every tree is ignited and survives with a PFT-specific fire resistance probability (cf. Thonicke
272 *et al.*, 2001) which is the same for all individuals that belong to the same PFT. In the patch
273 burnt, all litter carbon is combusted completely.

274 In boreal forests, evergreen trees exhibit water stress in spring, when relatively high air
275 temperature increases evaporative demand, while the soil is still frozen and thus limits the
276 water availability in the soil. This water stress forces evergreen trees to shed their needles
277 and making them less competitive against BL-S trees which might have their bud burst later
278 in the year. To correctly balance competition between B-NL and BL-S in boreal forests, we
279 increased the root-distribution factor β_{root} for B-NL trees from 0.943 (Schaphoff *et al.*,
280 2018b) to 0.965, which allows B-NL to reach deeper, non-frozen layers during spring thereby
281 preventing them from leaf senescence.

282 2.2 Model input data, simulation protocol and validation sites

283 Climate and soil data input

284 LPJmL-FIT uses air temperature [°C], precipitation [mm/d] and radiation (short-wave down
285 and long-wave net radiation [W/m²]) of the combined dataset of the WATCH (Weedon, 2011)
286 and WFDEI (Weedon, 2014) datasets at daily resolution on a 0.5° x 0.5° longitude-latitudinal
287 grid. This climate data set is based on the reanalysis of ERA-Interim, where precipitation
288 was bias-corrected using the Global Precipitation Climatology Centre data set (GPCC,
289 Schneider *et al.*, 2011). The climate data range from 1901 to 2013 with WFD covering 1901
290 to 1978 and WFDEI-GPCC is used from 1979 onwards. The atmospheric CO_2 concentration
291 is held constant at 296 ppm over the whole time period.

292 Soil texture is needed as model input and was taken from the Harmonized World Soil
293 Database (HWSD) version 1.2 (Nachtergaele & Montanarella, 2009). The soil depth was
294 kept constant at 2m for all grid cells. Our simulation domain covers Europe from 11°E to
295 36°W and 29.5°N to 62°N.

296 Simulation protocol

297 Model simulation starts from bare-ground and simulates a spin-up period of 500 years by
298 recycling the first 30 years of the climate data set (1901-1930) to bring natural vegetation
299 composition (here individual trees with their individual trait combinations) and all living and
300 dead carbon fluxes into equilibrium with the spin-up climate. We then performed a transient
301 run simulating potential natural vegetation until the end of 2013, i.e. without land use. For the
302 European simulation domain, 1000 forest patches being equivalent to 10 ha of forest area
303 are simulated in each grid cell where all patches receive the same climate data and the
304 same soil data as model input. Respective model output is then aggregated over all
305 simulated patches within a grid cell.

306 To allow for a detailed analysis of plant trait distribution, functional diversity and productivity,
307 we chose six different sites across Europe with near-natural forest stands and which cover a
308 broad range of climates (Table S4). Site-specific simulations follow the same protocol as
309 described above and were performed with 2500 patches at each site to ensure a higher
310 spatial coverage.

Model validation

312 Simulated seasonal and intra-annual GPP is validated against observed and remotely
313 sensed GPP data at six sites (Table S3) covering a climatic gradient (Table S4). We used
314 monthly MODIS remote sensing data (MOD17A2H) for the years 2004-2013 (Running,
315 2015) at six sites (see Table S1) and respective flux tower measurements from the Euroflux
316 network for the Laegeren (CH-Lae, D'Odorico, 2014; Paul-Limoges, 2018) and Hainich NP
317 (DE-Hai) (for general information, see Reichstein *et al.*, 2005; Papale *et al.*, 2006).
318 Simulated maps of vegetation height and biomass were evaluated against remotely sensed
319 products (Lefsky, 2007; Thurner, 2014). Details on the validation of GPP, vegetation height
320 and biomass are described in the SI. Simulated plant trait distributions were compared
321 against observed plant trait data from the TRY data base (Kattge *et al.*, 2011), see SI for
322 methods.

2.3 Computation of functional diversity indices

324 We quantified three complementary indices on multi-dimensional traits to describe FD,
325 namely functional richness (FR), functional divergence (FDv), and functional evenness (FE)
326 following Villéger et al. (2008) and Schneider et al. (2017), where each point represents one
327 tree individual (higher than 2m) with its unique trait combination. In this study, this
328 multidimensional trait space is based on SLA, LL, WD and tree height. While SLA, LL and
329 WD influence productivity and biomass (Reich, 2014) and therefore point to competitive
330 exclusion, tree height is regarded to describe niche differentiation (Garnier *et al.*, 2016). We
331 calculated the FD indices across and within PFTs to capture assembly processes across
332 meta-communities.

333 FR describes the extent of the occupied trait space and is calculated by the convex hull
334 volume including all points in that trait space, which is normalized by the maximum possible
335 trait volume. However, it implies that FR reacts strongly to outliers. FDv describes how far
336 environmental niches are separated and indicate the intensity of competitive interactions,
337 where FDv = 0 indicates convergent trait distribution due to strong environmental and
338 competitive filtering (Mason *et al.*, 2005; Villeger *et al.*, 2008). To measure FDv in a
339 multidimensional trait space, a sphere with radius $\overline{dG}$ centred in the trait cloud is calculated.
340 FDv then quantifies *how* points (trait combinations of trees) scatter relative to the surface of
341 the sphere (see eqs. 5-7 in SI and Fig. S1). If all points are located on the sphere, FDv
342 becomes unity independent on the respective distribution on the sphere. The more the index
343 decreases, the wider the points are spread around (inside and outside) the sphere. FDv
344 therefore quantifies how the occupied niches are separated. FE describes how regularly
345 points are distributed in the trait space, i.e. how efficient available resources are used

346   through niche occupation. FE is based on the minimum spanning tree (MST) linking all
347   points in the trait space in such a way, that the sum of all branches becomes minimal (see
348   equ. 11-13 in SI and Fig. S1). Therefore, FE increases when a) the points are evenly
349   distributed, i.e. having equal branch length; or b) the trait combinations of the trees are
350   equidistant in the trait space (Villeger *et al.*, 2008). Further details on FE, FDv and FR
351   quantification are provided in the SI.

352   Each index was computed by considering all trees as evenly weighted. Before calculation,
353   traits were normalized to their minimum and maximum observable values in the TRY sites in
354   Europe, thus ranging between 0 and 1. For each grid cell we checked that no dimensional
355   reduction was required by using the function "dbFD" of the R-package "FD" performing a
356   principal coordinates analysis (Laliberté, 2014). Due to constrained computation capacity,
357   we calculated all FD indices separately in groups of 50 patches in each grid cell (for which
358   1000 patches were simulated in total) and aggregated them to the grid level by using the
359   arithmetic mean. To visualize the stochastic uncertainty of the model, we calculated the
360   coefficient of variation (COV) of each index in a grid cell out of the groups of 50 patches
361   (n=20). Since all of these groups in a cell received the same climate data, the COV can be
362   seen as a measure for the stochastic uncertainty of the model.

363   3. RESULTS

364   3.1 Climate influence on trait distribution, productivity and tree
365   height

366   Environmental and competitive filtering allows those trees to establish and survive whose
367   trait combinations are suitable for local climate conditions in the forest patches simulated by
368   LPJmL-FIT. Unsuitable or less suitable trait combinations lead to a low growth efficiency and
369   are therefore outcompeted. The combination of climate suitability and competeveness has
370   the effect that the continuous, uniform distribution with which the model is initialized results
371   in a normal trait distribution at the local scale. The resulting trait distributions therefore
372   emerge from the LPJmL-FIT modelling framework (Fig.1). We compare simulated SLA and
373   WD against TRY observations for BL-S, BL-E trees and needle-leaved evergreen, i.e. B-NL
374   and T-NL trees (Fig. 2). Simulated mean trait distributions match the TRY observation
375   reasonably well for both, SLA and WD, for BL-S, BL-E and the two needle-leaved PFTs
376   (dashed lines in Fig. 2). Simulated ranges of SLA, however, are smaller than the original trait
377   range (see Table S2) and smaller than observed SLA (Fig.2). LPJmL-FIT simulates a mean
378   SLA of 16.11 with a standard deviation of +-1.25 mm²/mg for BL-S compared to 14.95 +-
379   6.09 documented in TRY. The simulated range for SLA is also smaller for BL-E (LPJmL-FIT:
380   9.31 +- 1.13 mm²/mg; TRY: 6.95 +- 2.72 mm²/mg) and the needle-leaved evergreen
381   (LPJmL-FIT: 6.11 +- 0.95 mm²/mg; TRY: 6.95 +- 2.72 mm²/mg). Simulated ranges for WD
382   are quite close to observed ranges in TRY for BL-S, slightly smaller for BL-E, but broader for
383   the needle-leaved PFTs (Fig. 2, bottom row).

384　The combined effects of environmental filtering and plant competition for light and water in
385　LPJmL-FIT also result in reasonable seasonal and interannual productivity (gross primary
386　productivity, GPP) as observed on six selected sites. The model quality is shown by a high
387　Pearson's R (≥0.89) and low NMSE (0.03 to 0.29; see Table S3, Fig. S2 and SI for details on
388　the evaluation methods and results, sites are described in Table S4). The simulated
389　competition between tree individuals results in closed forest cover and corresponding high
390　biomass storage in temperate and boreal forests (Fig. S3). We found simulated vegetation
391　height and biomass to compare well against remotely sensed observations and local in-situ
392　data, although the comparison of natural forest and actual vegetation is limited as remote-
393　sensing products detect properties of actual vegetation cover which are influenced by
394　current land-use and forest management (see SI for details on the evaluation method and
395　results). Centuries of land clearing, agricultural and forestry have greatly changed land cover
396　and reduced natural forests to few remaining small areas (Ellis *et al.*, 2013), which further
397　complicates the evaluation of simulated potential natural vegetation.

3.2 Climate influence on trait distributions within and across PFTs

400　Spatial distribution of simulated fractional cover of each PFT result from the PFT-specific
401　phenology and functional trait combinations, which determine the suitability of each
402　parameter set to the climate and soil conditions in a given grid cell (cf. Fig.1). Tree
403　individuals with trait combinations adapted to current climate are the most competitive and
404　most productive in sites with limited environmental stress severity (while their productivity
405　may decrease at stressed sites (Zhang *et al.*, 2018), and thus cover larger proportions of a
406　given grid cell (Fig. S4). The most suitable combination, to shed leaves under cold and/or
407　dry climate conditions, results in BL-S dominating central Europe, even though it also occurs
408　- albeit at much smaller fractions- in the boreal and the Mediterranean forests. B-NL
409　dominates northern Europe, and T-NL the Mediterranean basin, where it co-occurs with BL-
410　E. Several PFTs co-occur in the Mediterranean forests (3 tree PFTs and C_3 grasses) while
411　temperate forests in lowland Europe are dominated by just one tree PFT (Fig. S4). Note that
412　in all cases, the tree individuals still vary in their trait combination within each PFT.

413　Abiotic conditions, here aggregated to MAT [°C] and MAP [mm], are strongly linked to tree
414　establishment (Fig. 3). The climate space occupied by trees across all PFTs converges
415　towards higher MAT and lower MAP. Intra-PFT variation in SLA values decreases with
416　warmer and drier conditions. Most SLA variation, however, happens between PFTs that
417　occupy different parts of the climate space (Fig. 3a). The SLA of BL-S varies from values
418　around 13 mm²/mg under warmer and drier climate conditions to >20 mm²/mg in colder
419　climate conditions (<7°C) with a wide range in precipitation (500 to >2000 mm MAP). BL-S
420　co-exists with B-NL in cold/wet climate conditions, with BL-E in warmer and increasingly
421　drier climate conditions (>10°C MAT and 300 to 2000 mm MAP). Although many trait
422　combinations are possible under the "everything-is-everywhere" approach of LPJmL-FIT,
423　BL-S with SLA values lower than 13 mm²/mg do not occur despite a possible minimum of 7
424　mm²/mg (see Table S2). BL-E cover a similar temperature range as BL-S, but occur across

425 a wider SLA range between a MAT of 8 to 17°C, although the possible SLA range of BL-E is
426 among the smallest of all simulated PFTs. Again, this realized trait space separates these
427 PFTs clearly from the two needle-leaved PFTs, T-NL and B-NL, where T-NL increasingly
428 dominates at MAT>10°C and MAP<1000mm with SLA ranging from 5 to 8 mm²/mg, whereas
429 B-NL shows lowest SLA values at a MAT below 10°C (see Fig. 3a; Fig. S5 shows PFT-
430 specific SLA maps).

431 Simulated mean WD clearly separates along climate gradients across all PFTs (Fig. 3b).
432 Low WDs are simulated in cold climate conditions, and WD increases with increasing MAT
433 and decreasing MAP. B-NL and BL-S cover the WD space between 0.5 and <0.7 g/cm³
434 below 10°C MAT. WD around 0.7 g/m³ are found in cold (<10°C MAT) and drier climate
435 conditions (<1000 mm MAP), with similar WD values found in warmer (10-12°C MAT) and
436 wetter (>1000 mm MAP) climate conditions. Highest WD values (>1.1 g/cm³) are simulated
437 for T-NL, BL-S and BL-E with >15°C MAT and <1000 mm MAP (Fig. 3b). Higher WD allows
438 slow plant growth and lowers tree mortality risk (eq. 2 in 2.1) which explains why high WD
439 are simulated across all PFTs under dry climate conditions (see also Fig. S6 for PFT-specific
440 WD maps).

3.3 Functional diversity emerging from climate and plant competition

443 The calculation of all diversity indices is based on the initial 4-dimensional trait space out of
444 SLA, LL, WD and tree height. However, for visualisation, we remapped the trait space from
445 four dimensions to a three dimensional trait space composed of SLA, WD and tree height.
446 We plot the position of each tree individual in the trait space for the climatological different
447 sites Seitseminen, Laegern and Dundo (Fig. 4, left column). The occupied trait space forms
448 the hypervolume, i.e. the FR (shown in grey-blue in Fig. 4, 2nd column) for each site. The
449 sphere around the centre of gravity (grey surface and green cross, respectively shown in
450 Fig. 4, 3rd column) illustrates site-specific FDv, while FE is quantified from the minimum
451 spanning tree (Fig. 4, last column). Table S4 shows the site-specific FD indices for the six
452 sites.

453 The wide bi-modal distribution of SLA between BL-S and B-NL trees in Seitseminen
454 increases the trait space, i.e. FR, whereas in Laegern and Dundo simulated SLA
455 distributions show narrower bi-modal distributions or even converge (see density distribution
456 in Fig. 4, left column). Niche separation (FDv) and regularity of niche occupation (FE) are
457 more comparable across the three sites (Table S4). FDv is highest in Dundo, because points
458 in trait space lay closer to the surface of the sphere compared to Seitseminen and Laegern
459 (notice points outside the sphere in Seitseminen and Laegern). Compared to Laegern, we
460 find slightly higher FDv in Seitseminen, because of the divergent SLA distribution. Niche
461 occupation is less regularly distributed (FE) in Dundo compared to Seitseminen and
462 Laegern, because the trait space of B-NL trees is less occupied in Dundo, leading to larger
463 path length in between points of this PFT (SI, Fig. S1). This leads to more irregular distances
464 in between points, which lowers FE.

When calculating the FD indices for each PFT trait space separately and for each site, FDv and FE are similar to the corresponding across-PFT values (Table S5 and SI for computation of within-PFT FD indices). Within each PFT, diverse functional strategies co-exist, i.e. the intensity of plant competition and regularity of niche occupation is comparable to the one across PFTs. Specifically, FDv is high at Seitseminen for B-NL trees compared to the overall FDv, because the point cloud is clearly separated along the tree-height niche axis and shows a wider WD distribution compared to the other sites (Fig. 4, left column). However, intra-PFT FR is three orders of magnitude lower than FR across PFTs. This is mainly caused by a much lower realized trait space for LL (e.g. BL-S) and SLA (e.g. B-NL, see Fig. 4), while the intra-PFT range of tree heights and WDs is similar to that between PFTs. In summary, environmental and competitive filtering influence niche occupation in a similar way within as well as across PFTs.

3.4 Functional diversity at the European scale

At the European scale, spatial gradients in FD indices are relatively small and a few spatially distinct patterns stand out (Fig. 5). FR increases with the number of PFTs present through which the size of the trait space increases (Fig. 5a, compare Fig. S4). Higher FR is found in mountain areas throughout the continent, in boreal forests but also on the British Isles. Where B-NL and BL-S occupy distant parts of the trait space, FR reaches its maximal values of 0.03 to 0.04, very much alike in the Seitseminen site (compare Fig.4, top row). In contrast, lowest FR values are computed for areas where one PFT is dominant, especially in the lowland areas of temperate forests which are dominated by BL-S trees (Fig. 5a). The coefficient of variation (COV) for FR is high in temperate and alpine forests, where mean FR is low, because variability increases where the mean of a variable is close to zero. On the contrary, low values are found in Mediterranean and boreal forests (Fig. S7).

Functional Divergence is high in natural forests reaching values between 0.68 and 0.82 (Fig. 5b). Where needle-leaved and broad-leaved trees co-exist (cf. Fig. S4), FDv is higher, i.e. in boreal and mountain forests, and in southern Mediterranean forests. Where only one PFT dominates, FDv is lower (0.7-0.73 compared to >0.75), e.g. in lowland temperate and Mediterranean forests. In the transition zone to boreal forests or mountain forests, trait distributions of BL-S-dominated forests further converges (FDv ~0.68). Here, intensity of filtering increases (FDv converges) when climate conditions reduce growth efficiency of BL-S trees. Further north, growing conditions for B-NL are more suitable, allowing establishment of another plant strategy causing an increase in FDv (Fig. 5b). In contrast, in the southern Mediterranean forests, needle-leaved and broad-leaved trees are smaller (Fig. S3) and in competition with grasses for water, thus FDv is higher again (~0.76, see Fig. 5b). COV of FDv is generally very low with maximum values found in some mountainous and boreal transitional areas (Fig. S7).

Functional Evenness follows a different spatial pattern across Europe than the other two indices (Fig. 5c). Lower FE values (~0.72) are found in lowland temperate forest in central and eastern Europe as well as in the transition zone to the boreal forest in north-eastern Europe, where BL-S dominate but still grow in competition with B-NL trees (Fig. S3). FE

506 increases where only one NL-PFT dominates (e.g. British Isles, Norway) and is high in wet
507 Atlantic and in southern Europe, where high environmental stress results in efficient
508 resource use. Here, COV of FE corresponds to the spatial gradient of mean FE, maximum
509 COV is found where mean FE is lower (Fig. S7).

510 4. DISCUSSION

511 4.1 Effect of environmental and competitive filtering on trait
512 distribution and productivity

513 The adapted LPJmL-FIT model is capable of reproducing observed GPP with a small
514 modelling error and high correlation with observed data (see SI). Biomass and plant height
515 follow spatial distribution of previous publications (Thurner, 2014; Healey *et al.*, 2015),
516 although the comparison is limited by the long-term land-use history in Europe which
517 restricts the comparability between simulated and observed data and may explain the
518 discrepancy found. Simulated SLA and WD are in close agreement with observed TRY data.
519 These results show that the new version of LPJmL-FIT reproduces the spatial PFT and local
520 trait distributions as well as the productivity and biomass of European natural forests. Even
521 though a preference for measuring short-lived, broad-leaved species can influence
522 measured trait data which could overestimate, e.g., SLA (Sandel *et al.*, 2015), such bias is
523 found to be small for European trees and should have little influence on our results because
524 LPJmL-FIT clearly separates between broad-leaved and needle-leaved trees and focuses on
525 trees only. The model is capable of simulating potential natural vegetation without
526 prescribing the spatial extent of PFTs via bioclimatic limits and without prescribing the
527 functional traits in question (e.g. SLA, LL, WD). Therefore, it enables to investigate the
528 interaction between environmental and competitive filtering in European natural forests in an
529 unprecedented manner.

530 Simulated ranges for SLA (BL-S and BL-E) and WD (BL-E and needle-leaved trees) are
531 smaller than observed (Fig. 2 and Table S2). Heat and drought stress as well as light
532 availability (seasonal, vertical canopy structure) influence growing conditions of trees. These
533 climate factors act as environmental filter favouring plant strategies that are adapted to the
534 local climate. Tree growth efficiency influences tree competiveness and its capacity to reach
535 the top-layer in the canopy and gain most light in temperate and boreal forests. Therefore,
536 competitive filtering is the second driver of trees surviving and growing in a forest patch.
537 Additional processes not yet explicitly captured by LPJmL-FIT might explain the remaining
538 trait variability and include: i) dispersal and adaptive responses (incl. phenotypic plasticity of
539 traits), ii) nutrient availability (e.g. nitrogen limitation), iii) variable rooting strategies and
540 disturbances other than fire (Douma *et al.*, 2012; Van Bodegom *et al.*, 2012), and iv) trade-
541 offs between different trait combinations and species capacities to tolerate multiple
542 environmental stresses simultaneously (Niinemets & Valladares, 2006; Laanisto &
543 Niinemets, 2015). While the influence of adaptive responses on trait distribution is perhaps
544 difficult to measure, including nutrient availability would introduce another niche axis and

545   perhaps differentiate the trade-off with SLA in the LES better. Variable rooting strategies
546   could alleviate water stress in seasonally dry environments and increase growth efficiency,
547   hence tree height of Mediterranean forests (cf. Fig. S3). We have included fire disturbance in
548   LPJmL-FIT, which simulates high fire activity in the Mediterranean forests, less in boreal and
549   low fire activity in temperate forests, but other disturbance agents such as wind-throw or
550   frost could also further diversify plant strategies, and thus increase the width of the simulated
551   trait distribution. Implementing these disturbances into LPJmL-FIT would be expected to
552   decrease the competitiveness of the BL-S trees in boreal and mountainous forests, and thus
553   further restricting their spatial extent.

554   Specific model functions determine the model outcome. The phenology parameter (Table
555   S1) influence GPP, growth efficiency, and thus the performance of a tree in the forest patch.
556   In exchange with climate conditions, the phenology parameters determine the spatial
557   distribution of the PFTs, including grasses. The trade-off between SLA and LL defines the
558   carbon cost for leaves (or needles) under specific climate conditions which then determine
559   the length of the growing season, and thus vegetation productivity. With more SLA and LL
560   measurements available for temperate forests this relationship could be adjusted and
561   contribute to further reduce modelling error of the simulated trait distribution (Fig.2). The
562   WD-dependent mortality function (see equ. 2) influences simulated biomass, more data on
563   WD and tree mortality would help to improve parameterisation of this function. Further
564   reductions in the model error of simulated WD distribution, tree height and biomass could be
565   expected.

566   Plant-trait validation would profit from more and better resolved plant trait measurements in
567   natural forests in Europe. In this study, we had to aggregate several TRY sites and also to
568   merge T-NL and B-NL to validate simulated trait distribution. Ideally, trait measurements at
569   FLUXNET sites, where we can evaluate both productivity and plant traits, would allow high
570   resolution and in-depth model evaluation. With these consistently measured data available,
571   model evaluation could be extended to water fluxes and biomass as well as stand structure
572   and their related plant traits. Alternatively, remotely sensed traits which are already available
573   at the Laegern site (cf. Schneider *et al.*, 2017) or emerging from global remote-sensing
574   mission (cf. Jetz *et al.*, 2016) could be used in the future. However, cross-validation
575   experiments are required to compare spatially continuous traits observed from remote
576   sensing to traits simulated by DGVMs using flexible-individual traits, but approaches are
577   underway (cf. Garonna, 2018; Lausch, 2018). Simulated trait maps for SLA and WD can be
578   validated against interpolated observed trait maps (Butler *et al.*, 2017; Šímová *et al.*, 2018),
579   even though observed trait distributions include those from highly managed forests.
580   Interpolated trait maps, which combine plant trait data with actual species' presence data,
581   can lead to a potential bias in data-model comparison because species are planted in
582   managed forests. Generating trait maps which use potential natural species distribution
583   would improve such data-model comparison because they would be closer to the spatial trait
584   distribution that would result from environmental and competitive filtering. Model-data
585   comparison could be improved with a) more trait data being extracted in natural vegetation
586   and extrapolated using species distribution data to the continental scale; and b) allowing for
587   a better overlap of observed vs. simulated plant traits such as leaf N (observation available

588 but simulated map missing) or wood density (observation missing, but simulated map
589 available).

4.2 Community-assembly effects on traits and functional diversity across Europe

592 Community assembly at a site results from dispersal or migration, environmental filtering of
593 trait combinations adapted to local climate and finally plant competition (Bernard-Verdier *et*
594 *al.*, 2012). In the adapted LPJmL-FIT model, trait combinations are drawn from observed
595 ranges for SLA and WD. It principally means that any conceivable trait combination can
596 establish everywhere at any time for every PFT without explicitly considering trait inheritance
597 or seed dispersal. Currently, surviving trait combinations in the model represent those trees
598 whose traits are best suited to local climate and the competitive conditions in the established
599 tree community. Therefore, environmental filtering interacts with competitive filtering and
600 reproduces observed trait distributions and productivity of natural forests. Scaling up to the
601 whole study region, SLA and WD gradients emerge along climatic gradients and reflect
602 variability in trait ranges.

603 Simulated SLA cover a wide temperature and precipitation range, separated by SLA ranges
604 as observed for the 4 PFTs in Europe. Where cold temperatures and light increasingly limit
605 productivity, i.e. in the boreal zone, simulated SLA for BL-S increases, meaning trees with
606 extremely high SLA and short LL survive cold winters and grow in short summers. The shift
607 towards higher WD in southern Europe indicates a local adaptation to seasonally dry
608 Mediterranean-type climate. Generally, the increasingly dry climate filters higher WD for BL-
609 E and T-NL which indicates better adaptation to drought.

610 The identified spatial FD patterns reflect the combined effect of environmental and
611 competitive filtering. The influence of climate on surviving plant strategies and their
612 coexistence are reflected in the occupied trait space. FR is high where trait clusters of
613 different PFTs are distant and thus cover a large volume of the trait space, which is the case
614 in high-elevation areas and the boreal zone, where BL-S and B-NL co-exist. Here, BL-S
615 adapt to high SLA values and lower LL, because of shorter vegetation periods leading to a
616 wider functional gap in these two traits between BL-S and B-NL trees. FR is small where
617 only BL-S trees dominate the patches of temperate forests (Fig. 5). Here, trait variation is
618 small in each of the traits used, specifically LL, thus resulting in a small trait space, whereas
619 the ranges of WD and tree height do not change substantially. In the Mediterranean region,
620 where the trait space covered by each PFT is larger, FR is comparable to temperate forests.
621 Although the coexistence of up to 4 PFTs would lead to a relatively high FR in leaf traits in S-
622 Europe, lower tree heights limit trait space and counteract the effect of diverse leaf
623 strategies. In the southern Mediterranean, where tree growth reaches its limits, FR
624 decreases because few niches can be occupied under the dry climate conditions.

625 Functional divergence describes the diversity of co-existing functional strategies. A high FDv
626 illustrates a high degree of niche differentiation, thus high competitive exclusion or intense
627 competitive interaction (Mason *et al.*, 2005; Villeger *et al.*, 2008; Garnier *et al.*, 2016). The

628   larger the influence of environmental filtering through abiotic stress, the more the trait
629   distribution converges (Bernard-Verdier *et al.*, 2012). Maps of FDv (Fig.5) therefore illustrate
630   the relative strength of environmental vs. competitive filtering on trait composition. Where
631   climate allows needle- and broad-leaved trees to co-exist (in mountains, boreal forests, wet
632   temperate and Mediterranean forests), FDv is high because of the distant SLA distribution of
633   BL-S and B-NL. In Mediterranean and temperate climates, SLA distributions converge more,
634   and FDv declines slightly to values around 0.7 (Fig.5b). Interestingly, FDv declines further in
635   the transition from temperate forests to boreal and to mountain forests, respectively. Being
636   dominated by BL-S, the performance of these trees declines as climate gets colder, thus the
637   abiotic stress increases which leads to a less divergent distribution. Further north (or at
638   higher elevation) the growing conditions for B-NL improve, thus their dominance increases
639   and increases FDv again. Physiological traits (SLA, WD, LL) converge at the transition from
640   temperate to boreal forests, indicating competitive exclusion. In contrast, in southern
641   Mediterranean forests, increasing drought stress reduces tree height and favours a wide
642   SLA range and higher WD (Fig. 3, S5). In the northern mountain ranges, T-NL, BL-S and B-
643   NL co-exist, each with different SLA and WD. T-NL and B-LE with SLA and WD close to
644   each other dominate the lowland and coastal area, resulting in lower FDv. The distributions
645   diverge again further south with increasing drought stress, promoting co-occurring
646   alternative strategies (Fig. 5b, S3). We find that such bi-modal changes in FDv reflect shifts
647   between competitive exclusion, linked to physiological traits (SLA, WD, LL), and niche
648   differentiation, linked to morphological traits (tree height).

649   Functional evenness quantifies the regularity of the distribution in the trait space, i.e. niche
650   occupation (cf. Mason *et al.*, 2005; Villeger *et al.*, 2008) and could be interpreted as a lower
651   utilization of resources due to the more irregular occupation of the trait space, i.e.
652   environmental niches (cf. Mason *et al.*, 2005). However, there are few studies which have
653   investigated the changes of FE along climatic gradients. Recent studies focussed on
654   changes in FE along disturbance gradients (e.g., Mouillot *et al.*, 2013) and at the local scale
655   (Pakeman, 2011). We find high FE in areas where dry and cold climate conditions limit tree
656   growth and under wet (Atlantic) conditions. Increasing disturbances (fire) and climatic stress
657   (drought) increase resource-use efficiency as suggested by Pakeman (2011). In highly
658   stressed environments, no strategy can dominate, thus functional traits are more evenly
659   distributed. Low FE is found in mixed temperate forests and in the transition from temperate
660   to boreal forests, where BL-S and B-NL occupy distant parts of the trait space. At the Pan-
661   European scale, FE does not follow a unique climatic gradient which could be interpreted as
662   habitat filtering as suggested by Pakeman (2011). In our study, it is rather a combination of
663   environmental and competitive filtering within and across PFTs.

664   We computed FR, FDv and FE from four traits following the approach of Villeger et al. (2008)
665   as implemented for the Laegern site in Schneider *et al.* (2017). The FD indices change with
666   the traits considered and the dimensionality of the trait space. At the Laegern site, we
667   compute FR values one order of magnitude lower than published in Schneider *et al.* (2017)
668   because we calculate FR for a 4- instead of a 3-dimensional trait space. In contrast, we
669   derived comparable FDv and slightly lower FE values for the Laegern site (Schneider *et al.*,
670   2017). A direct comparison between remotely sensed and simulated FD based on 3 traits is

671   of interest and relies on directly comparable trait spaces and indices. Quantification of FD

672   indices strongly depend on the type of traits (physiological vs. morphological) and the

673   context of their interpretation, e.g. niche differentiation or ecosystem function to which the

674   considered traits relate. Comparing site-specific FD indices based on similar traits where

675   also trait observations are available would be a great step forward to evaluate site-specific

676   FD and its changes along climatic gradients at the regional as well as continental scale.

677   Model-data comparison can help to further investigate the importance of spatial scale or

678   abiotic gradients at the landscape scale, where DGVMs with flexible individual traits such as

679   LPJmL-FIT can be used to test and explore respective FD hypotheses to advance

680   biodiversity-ecosystem function theory (Hisano *et al.*, 2018).

681   Trees occupy trait ranges within each PFT allowing different PFTs to co-exist as a result of

682   functional diversity, tree demography and disturbance in all biomes. Site-specific water

683   availability and temperature have been shown to influence functional composition in

684   temperate forests emphasizing the importance to investigate functional diversity along

685   climate gradients (Zhang *et al.*, 2018).

686   We find high functional diversity in European natural forests not only for temperate forests as

687   found by Liebergesell *et al.* (2016) but also for boreal and Mediterranean forests. The

688   simulated community assembly of European biomes can be explained by the interplay

689   between environmental and competitive filtering: I) In the boreal zone and in high-mountain

690   areas (e.g. Carpathian Mountains, Alps or the Pyrenees) the growing season is short, and

691   needle-leaved trees (low SLA) which keep their leaves longer (high LL) but grow relatively

692   fast due to low WD, are the dominant tree growth strategy mostly as a result of

693   environmental filtering. B-NL trees have high resistance to cold temperatures and their

694   evergreen strategy allows them to fully exploit the short growing season (see Table 1). In

695   contrast, broadleaved trees (BL-S), which are more prone to cold temperatures and have to

696   unfold their thin, short-lived leaves at the start of the growing season, have a disadvantage

697   under this climate. Nevertheless over a wide range within the boreal zone, B-NL trees are

698   accompanied by BL-S trees. This means, in this range environmental and competitive

699   filtering are not strong enough to select for B-NL trees only and both growing strategies can

700   co-exist. Competitive filtering though pushes BL-S towards lower LL and higher WD as in the

701   temperate zone, which minimizes the overlap of trait values between the two PFTs (Fig. 1).

702   Due to the BL-S and B-NL co-existence a wide trait space (high FR) is covered in which trait

703   combinations are mostly evenly spaced (high FE) and divergent (high FDv), allowing for

704   relatively high resource-use efficiency. The same effect applies further South towards the

705   temperate zone, where B-NL trees can still be found in mixed temperate forests.

706   II) In the temperate zone, climate supports a longer growing season, higher productivity and

707   biomass. Here, BL-S trees dominate due to competitive filtering. Their tolerance of warmer

708   temperatures together with low carbon investment in short-lived and thin leaves (Table 1)

709   makes this PFT very competitive along a large climate gradient. Moreover, towards warmer

710   and drier climate conditions, the WD of BL-S trees increases in order to survive this climatic

711   stress keeping this PFT dominant. The clear PFT dominance decreases FR, and leads to

712   intermediate FE and FDv. Towards the Mediterranean zone new tree growth strategies (BL-

713 E, T-NL) enter the forest community with milder winter and drier summer changing
714 environmental filtering effects.

715 III) In the Mediterranean zone forests are stressed by drought and warm temperatures,
716 therefore limitations of growing conditions vary and environmental filtering plays an important
717 role. BL-E and T-NL trees with low SLA and high WD are adapted to seasonally dry
718 summers and can therefore co-exist in complementary and regularly spaced niches which
719 confirms previous findings (Carnicer *et al.*, 2013). Whereas BL-E trees tolerate warm
720 temperatures and drought, T-NL trees are specialists for warm, dry and fire-prone
721 environments (Table 1). Given those dynamic changes in niche occupation, FE and FDv are
722 high in mountainous areas and in the semi-arid southern Mediterranean areas. Where T-NL
723 dominate FDv is slightly lower, i.e. niche occupation being less diverse.

5. Conclusion

725 We introduce a new generation, large-scale vegetation model for Europe allowing to
726 dynamically simulate functional diversity on a continental scale, alongside with productivity
727 and tree demography. Approximating competition of individual trees with randomly selected
728 functional trait combinations has proven successful to reproduce trait patterns, productivity
729 and tree demography of natural forest ecosystems. Whereas some trait ranges are
730 constrained by PFTs (SLA), others follow similar climatic gradients across all PFTs (WD).
731 These results complement the current spatially non-contiguous data of trait distributions
732 derived from earth observation data, and allow large-scale estimates of functional diversity
733 across Pan-Europe. We demonstrate how functional richness, divergence and evenness
734 vary strongly across Pan-Europe and emerge from environmental and competitive filtering
735 alike. Co-existence of functionally diverse trees results from plant trait diversity, tree
736 demography and disturbance under varying strength of environmental and competitive
737 filtering.

6. ACKNOWLEDGMENTS

752   Technology, was under a contract with the National Aeronautics and Space Administration.

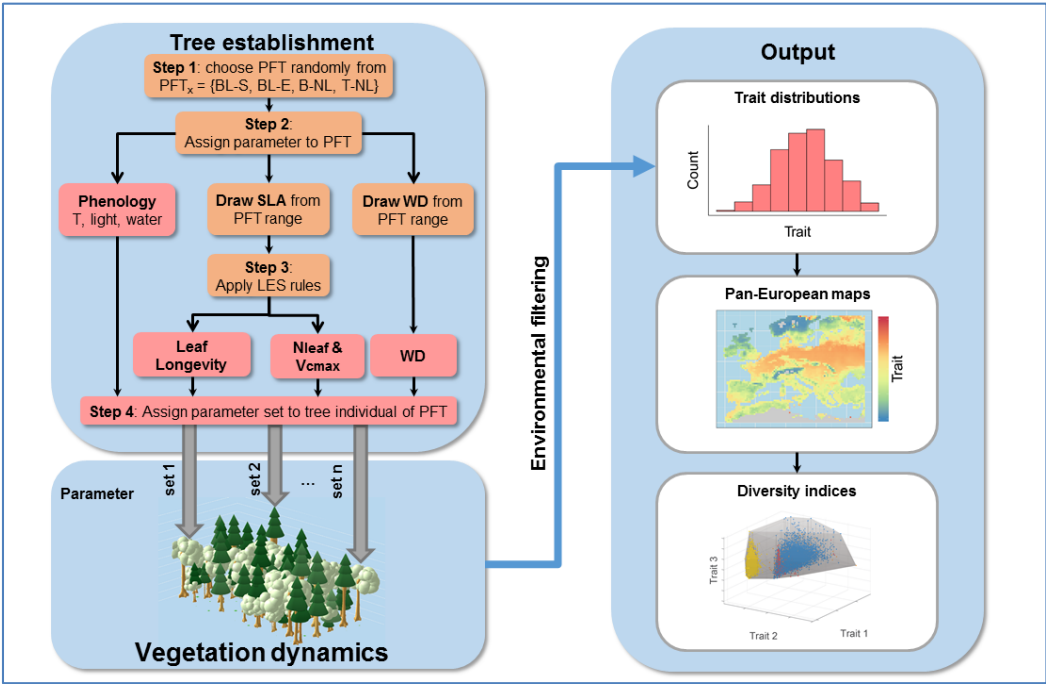753   Government sponsorship is acknowledged.

Figures

Figure 1 Conceptual scheme illustrating how flexible individual parameter are assigned to tree individuals belonging to a specific PFT, including LES (leaf–) and SES (stem–economics) plant traits in LPJmL-FIT. Parameter sets are assigned to individual trees at model initialization as well as gap opening. Climate, soil conditions and competition between individual trees within and across PFTs (environmental filtering) result in aggregated grid-cell trait distributions within patches. They are visualized as trait maps and are used to quantify diversity indices.
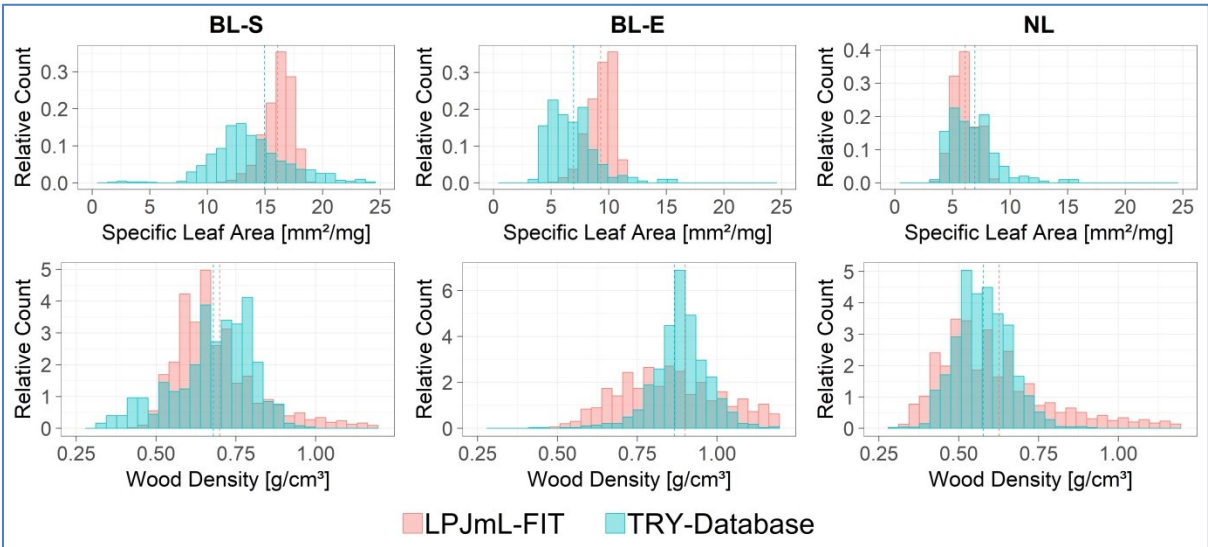

Figure 2 Trait distribution of Specific Leaf Area (top panel) and wood density (bottom panel) for broadleaved summergreen PFT (BL-S, left column), broadleaved evergreen PFT (BL-E, central column) and both, boreal and temperate, needleleaved evergreen PFTs (NL, right column) as simulated by LPJmL-FIT (light red) and observed by TRY data base entries (light cyan). Dashed vertical lines show the simulated (light red) and measured (light cyan) average trait values for each PFT.
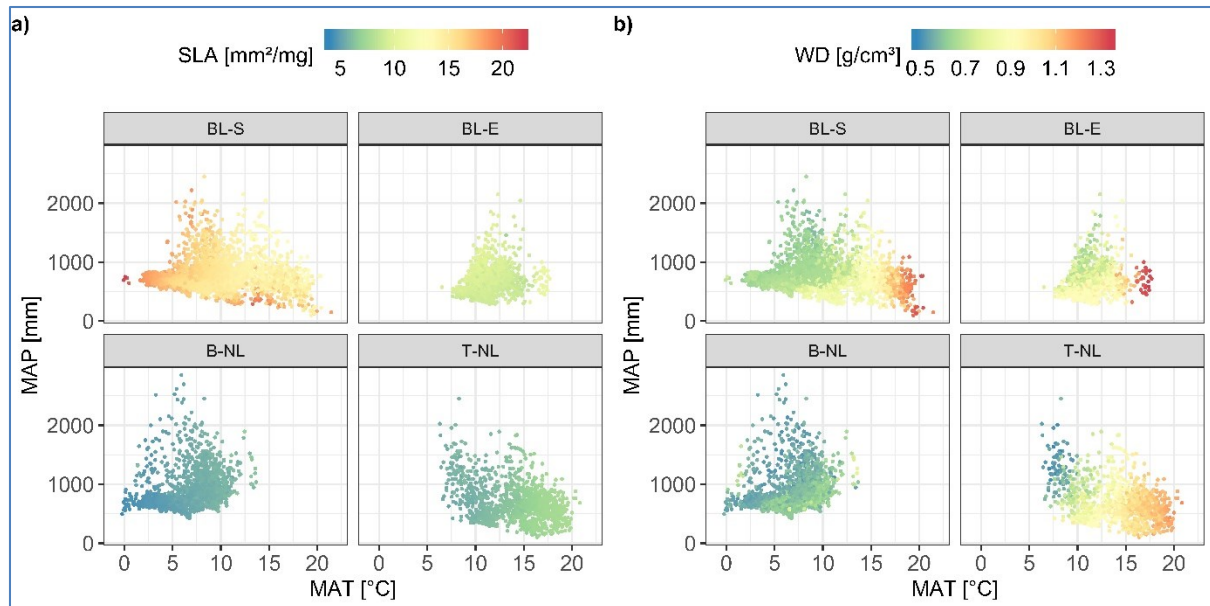
769

Figure 3 Mean Specific Leaf Area (SLA) and Wood Density (WD) distribution for each PFT plotted against mean annual temperature (MAT) and mean annual precipitation (MAP). The colour of each dot represents a mean SLA (a) and WD (b) value and each panel belongs to a PFT. (Broadleaved summergreen: BL-S; Broadleaved evergreen: BL-E; Boreal needle-leaved evergreen: B-NL; and Temperate needle-leaved evergreen: T-NL) Mean trait values are averaged over the 2004-2013 time period for 1000 patches per grid cell.
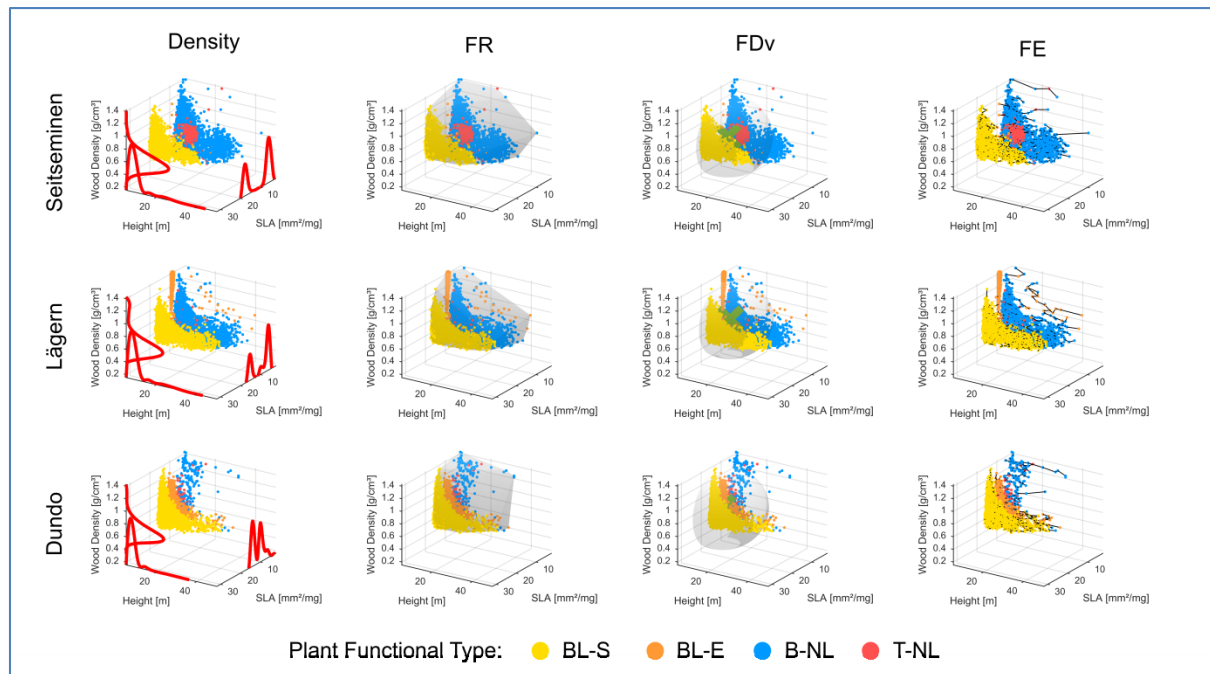

776

Figure 4 Distribution of simulated trees in a 3-dimensional trait space (Height, WD, and SLA). We plot density (far left) and functional diversity indices for 2'500 simulated patches (FR center left; FDv center right; and FE (far right) for three sites (Seitseminen (top row), Lägern (middle row) and Dundo (bottom row)). Ranges of the SLA and WD axes correspond to the maximum trait range across all PFTs used in the simulation (see Table S2). Seitseminen, Laegern and Dundo represent boreal, mixed temperate and Mediterranean-type forests, respectively. Each dot represents a trait combination of one tree larger than 5m while the colour indicates its PFT type. Plant Functional Types are: Broadleaved summergreen (BL-S), Broadleaved Evergreen (BL-E), boreal needle-leaved evergreen (B-NL); and temperate needle-leaved evergreen (T-NL).

22

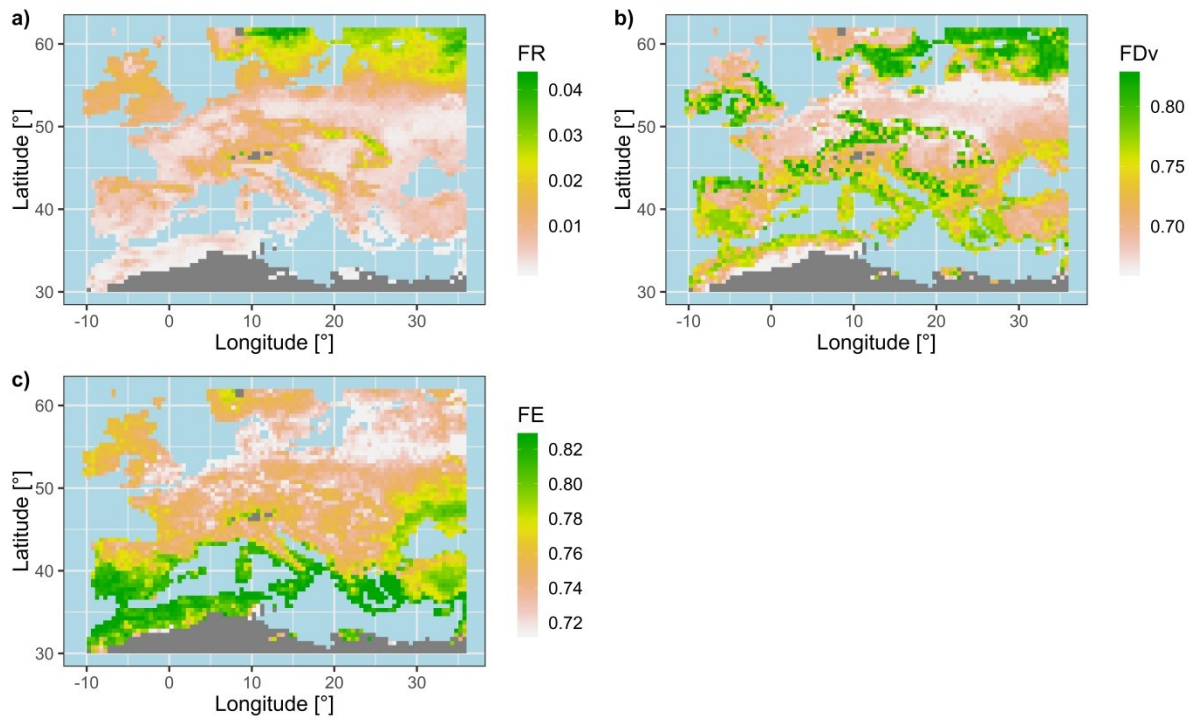Figure 5 Maps of functional richness (FR, panel a)), functional diversity (FDv, panel b)) and functional evenness (FE, c)). All three functional diversity indices are based on SLA, LL, WD and tree height averaged over all individual trees, which are at least 5m tall. Effects on FR, FDv and FE result from trait variability within and across PFTs present in 1000 patches in a grid cell.

786

787
788
789
790

791

23

Tables

PFT	Resistance to				Leaf strategy (SLA range, SLA-LL relation)	Growth strategy	Environment
	Cold temperature	Warm temperature	Drought	Fire			
BL-S	low	medium	low	low	Mostly thin and short-lived leaves	flexible WD, low WD in north, high WD in south	very flexible leaf strategy, but less specialized flexible growing strategy very competitive in temperate zone
BL-E	low	high	high	medium	moderate leaf cost intermediate leaf longevity	high WD in dry environment lower WD under wet conditions	less flexible leaf strategy conservative growing strategy competitive in warm temperate zones
B-NL	high	low	low	low	expensive and long-lived needles	fast growth, due to lower WD	conservative leaf strategy fast growing strategy specialist in cold climates with short growing season
T-NL	low	high	high	high	expensive and long-lived needles	high WD in dry environment, fast-growing under colder climate, and thus lower WD	conservative leaf strategy conservative growing strategy specialist in warm, dry and fire-prone environments

793   **Table 1 Overview of the PFT characteristics: phenology, fire sensitivity, leaf and growth strategy and environment**

794

7. REFERENCES

Bernard-Verdier, M., Navas, M.-L., Vellend, M., Violle, C., Fayolle, A., Garnier, E. & Cornelissen, H. (2012) Community assembly along a soil depth gradient: contrasting patterns of plant trait convergence and divergence in a Mediterranean rangeland. *Journal of Ecology*, **100**, 1422-1433.

Bohn, U., Zazanashvili, N. & Nakhutsrishvili, G. (2007) The Map of the Natural Vegetation of Europe and its application in the Caucasus Ecoregion. *Bulletin of the Georgia Academy of Science*, **175**, 112-121.

Bruelheide, H., Dengler, J., Purschke, O., Lenoir, J., Jimenez-Alfaro, B., Hennekens, S.M., Botta-Dukat, Z., Chytry, M., Field, R., Jansen, F., Kattge, J., Pillar, V.D., Schrodt, F., Mahecha, M.D., Peet, R.K., Sandel, B., van Bodegom, P., Altman, J., Alvarez-Davila, E., Arfin Khan, M.A.S., Attorre, F., Aubin, I., Baraloto, C., Barroso, J.G., Bauters, M., Bergmeier, E., Biurrun, I., Bjorkman, A.D., Blonder, B., Carni, A., Cayuela, L., Cerny, T., Cornelissen, J.H.C., Craven, D., Dainese, M., Derroire, G., De Sanctis, M., Diaz, S., Dolezal, J., Farfan-Rios, W., Feldpausch, T.R., Fenton, N.J., Garnier, E., Guerin, G.R., Gutierrez, A.G., Haider, S., Hattab, T., Henry, G., Herault, B., Higuchi, P., Holzel, N., Homeier, J., Jentsch, A., Jurgens, N., Kacki, Z., Karger, D.N., Kessler, M., Kleyer, M., Knollova, I., Korolyuk, A.Y., Kuhn, I., Laughlin, D.C., Lens, F., Loos, J., Louault, F., Lyubenova, M.I., Malhi, Y., Marceno, C., Mencuccini, M., Muller, J.V., Munzinger, J., Myers-Smith, I.H., Neill, D.A., Niinemets, U., Orwin, K.H., Ozinga, W.A., Penuelas, J., Perez-Haase, A., Petrik, P., Phillips, O.L., Partel, M., Reich, P.B., Romermann, C., Rodrigues, A.V., Sabatini, F.M., Sardans, J., Schmidt, M., Seidler, G., Silva Espejo, J.E., Silveira, M., Smyth, A., Sporbert, M., Svenning, J.C., Tang, Z., Thomas, R., Tsiripidis, I., Vassilev, K., Violle, C., Virtanen, R., Weiher, E., Welk, E., Wesche, K., Winter, M., Wirth, C. & Jandt, U. (2018) Global trait-environment relationships of plant communities. *Nat Ecol Evol*, **2**, 1906-1917.

Butler, E.E., Datta, A., Flores-Moreno, H., Chen, M., Wythers, K.R., Fazayeli, F., Banerjee, A., Atkin, O.K., Kattge, J., Amiaud, B., Blonder, B., Boenisch, G., Bond-Lamberty, B., Brown, K.A., Byun, C., Campetella, G., Cerabolini, B.E.L., Cornelissen, J.H.C., Craine, J.M., Craven, D., de Vries, F.T., Diaz, S., Domingues, T.F., Forey, E., Gonzalez-Melo, A., Gross, N., Han, W., Hattingh, W.N., Hickler, T., Jansen, S., Kramer, K., Kraft, N.J.B., Kurokawa, H., Laughlin, D.C., Meir, P., Minden, V., Niinemets, U., Onoda, Y., Penuelas, J., Read, Q., Sack, L., Schamp, B., Soudzilovskaia, N.A., Spasojevic, M.J., Sosinski, E., Thornton, P.E., Valladares, F., van Bodegom, P.M., Williams, M., Wirth, C. & Reich, P.B. (2017) Mapping local and global variability in plant trait distributions. *Proc Natl Acad Sci U S A*, **114**, E10937-E10946.

Cadotte, M.W., Carscadden, K. & Mirotchnick, N. (2011) Beyond species: functional diversity and the maintenance of ecological processes and services. *Journal of Applied Ecology*, **48**, 1079-1087.

Carmona, C.P., de Bello, F., Mason, N.W.H. & Leps, J. (2016) Traits Without Borders: Integrating Functional Diversity Across Scales. *Trends Ecol Evol*, **31**, 382-394.

Carnicer, J., Barbeta, A., Sperlich, D., Coll, M. & Penuelas, J. (2013) Contrasting trait syndromes in angiosperms and conifers are associated with different responses of tree growth to temperature on a large scale. *Front Plant Sci*, **4**, 409.

840 Chave, J., Coomes, D., Jansen, S., Lewis, S.L., Swenson, N.G. & Zanne, A.E. (2009)
841   Towards a worldwide wood economics spectrum. *Ecol Lett*, **12**, 351-66.

842 D'Odorico, P., Gonsamo, A., Pinty, B., Gobron, N., Coops, N., Mendez, E., & Schaepman,
843   M.E. (2014) Intercomparison of fraction of absorbed photosynthetically active
844   radiation products derived from satellite data over Europe. *Remote Sensing of*
845   *Environment*, **142**, 141-154.

846 Díaz, S., Kattge, J., Cornelissen, J.H.C., Wright, I.J., Lavorel, S., Dray, S., Reu, B., Kleyer,
847   M., Wirth, C., Colin Prentice, I., Garnier, E., Bönisch, G., Westoby, M., Poorter, H.,
848   Reich, P.B., Moles, A.T., Dickie, J., Gillison, A.N., Zanne, A.E., Chave, J., Joseph
849   Wright, S., Sheremet'ev, S.N., Jactel, H., Baraloto, C., Cerabolini, B., Pierce, S.,
850   Shipley, B., Kirkup, D., Casanoves, F., Joswig, J.S., Günther, A., Falczuk, V., Rüger,
851   N., Mahecha, M.D. & Gorné, L.D. (2016) The global spectrum of plant form and
852   function. *Nature*, **529**, 167-171.

853 Douma, J.C., Witte, J.-P.M., Aerts, R., Bartholomeus, R.P., Ordoñez, J.C., Venterink, H.O.,
854   Wassen, M.J. & van Bodegom, P.M. (2012) Towards a functional basis for predicting
855   vegetation patterns; incorporating plant traits in habitat distribution models.
856   *Ecography*, **35**, 294-305.

857 Ellis, E.C., Kaplan, J.O., Fuller, D.Q., Vavrus, S., Goldewijk, K.K. & Verburg, P.H. (2013)
858   Used planet: A global history. *Proceedings of the National Academy of Sciences of*
859   *the United States of America*, **110**, 7978-7985.

860 FAO (2018) Terms and Definitions FRA 2020. In: *Forest Resources Assessment Working*
861   *Papers* (ed. D.P.B.A. Pekkarinen.). FAO Forestry Department, Rome.

862 Forkel, M., Carvalhais, N., Schaphoff, S., von Bloh, W., Migliavacca, M., Thurner, M. &
863   Thonicke, K. (2014) Identifying environmental controls on vegetation greenness
864   phenology through model-data integration. *Biogeosciences*, **11**, 7025-7050.

865 Funk, J.L., Larson, J.E., Ames, G.M., Butterfield, B.J., Cavender-Bares, J., Firn, J., Laughlin,
866   D.C., Sutton-Grier, A.E., Williams, L. & Wright, J. (2017) Revisiting the Holy Grail:
867   using plant functional traits to understand ecological processes. *Biol Rev Camb*
868   *Philos Soc*, **92**, 1156-1173.

869 Garnier, E., Navas, M.-L. & Grigulis, K. (2016) *Plant Functional Diversity. Organisms, traits,*
870   *community structure, and ecosystem properties*. Oxford University Press, Oxford.

871 Garonna, I., de Jong, R., Stöckli, R., Schmid, B., Schenkel, D., David, S., & Schaepman,
872   M.E. (2018) Shifting relative importance of climatic constraints on land surface
873   phenology. *Environmental Research Letters*, **13**, 024025.

874 Geller, G.N., Halpin, P.N., Helmuth, B., Hestir, E.L., Skidmore, A., Abrams, M.J., Aguirre, N.,
875   Blair, M., Botha, E., Collof, M., Dawson, T., Franklin, J., Horning, N., James, C.,
876   Magnusson, W., Santos, M.J., Schill, S.R. & Williams, K. (2017) Remote Sensing for
877   Biodiversity. *The GEO Handbook on Biodiversity Observation Networks* (ed. by M.
878   Walters and R.J. Scholes), pp. 187-210. Springer Nature, Cham, Switzerland.

879 Hallik, L., Niinemets, Ü. & Wright, I. (2009) Are species shade and drought tolerance
880   reflected in leaf-level structural and functional differentiation in Northern Hemisphere
881   temperate woody flora? . *The New Phytologist*, **184**, 257-274.

882 Healey, S.P., Hernandez, M.W., Edwards, D.P., Lefsky, M.A., Freeman, E., Patterson, P.L.,
883   Lindquist, E.J. & Lister, A.J. (2015) CMS: GLAS LiDAR-derived Global Estimates of
884   Forest Canopy Height, 2004-2008. In: (ed. O. Daac), Oak Ridge, Tennessee, USA.

885 Hisano, M., Searle, E.B. & Chen, H.Y.H. (2018) Biodiversity as a solution to mitigate climate
886   change impacts on the functioning of forest ecosystems. *Biological Reviews*, **93**, 439-
887   456.

888 Hooper, D.U., Chapin, F.S., Ewel, J.J., Hector, A., Inchausti, P., Lavorel, S., Lawton, J.H.,
889   Lodge, D.M., Loreau, M., Naeem, S., Schmid, B., Setala, H., Symstad, A.J.,
890   Vandermeer, J. & Wardle, D.A. (2005) EFFECTS OF BIODIVERSITY ON
891   ECOSYSTEM FUNCTIONING: A CONSENSUS OF CURRENT KNOWLEDGE.
892   *Ecological Monographs*, **75**, 3-35.

893 Jetz, W., Cavender-Bares, J., Pavlick, R., Schimel, D., Davis, F.W., Asner, G.P., Guralnick,
894   R., Kattge, J., Latimer, A.M., Moorcroft, P., Schaepman, M.E., Schildhauer, M.P.,
895   Schneider, F.D., Schrodt, F., Stahl, U. & Ustin, S.L. (2016) Monitoring plant functional
896   diversity from space. *Nat Plants*, **2**, 16024.

897 Kattge, J., S. Díaz, S. Lavorel, I. C. Prentice, P. Leadley & G. Bönisch, E.G., M. Westoby, P.
898   B. Reich, I. J. Wright, J. H. C. Cornelissen, C. Violle, Harrison, S. P., , P. M. Van
899   Bodegom, M. Reichstein, B. J. Enquist, N. A. Soudzilovskaia, D. D. Ackerly, M.
900   Anand, O. Atkin, M. Bahn, T. R. Baker, D. Baldocchi, R. Bekker, C. C. Blanco, B.
901   Blonder, W. J. Bond, R. Bradstock, D. E. Bunker, F. Casanoves, J. Cavender-Bares,
902   J. Q. Chambers, F. S. Chapin Iii, J. Chave, D. Coomes, W. K. Cornwell, J. M. Craine,
903   B. H. Dobrin, L. Duarte, W. Durka, J. Elser, G. Esser, M. Estiarte, W. F. Fagan, J.
904   Fang, F. Fernández-Méndez, A. Fidelis, And B. Finegan, Flores, O., Ford, H., Frank,
905   D., Freschet, G. T., Fyllas, N. M., Gallagher, R. V., Green, W. A., Gutierrez, A. G.,
906   Hickler, T., Higgins, S. I., Hodgson, J. G., Jalili, A., Jansen, S., Joly, C. A., Kerkhoff,
907   A. J., Kirkup, D., Kitajima, K., Kleyer, M., Klotz, S., Knops, J. M. H., Kramer, K.,
908   Kühn, I., Kurokawa, H., Laughlin, D., Lee, T. D., Leishman, M., Lens, F., Lenz, T.,
909   Lewis, S. L., Lloyd, J., Llusià, J., Louault, F., Ma, S., Mahecha, M. D., Manning, P.,
910   Massad, T., Medlyn, B. E., Messier, J., Moles, A. T., Müller, S. C., Nadrowski, K.,
911   Naeem, S., Niinemets, Ü., Nöllert, S., Nüske, A., Ogaya, R., Oleksyn, J.,
912   Onipchenko, V. G., Onoda, Y., Ordoñez, J., Overbeck, G., Ozinga, W. A., Patiño, S.,
913   Paula, S., Pausas, J. G., Peñuelas, J., Phillips, O. L., Pillar, V., Poorter, H., Poorter,
914   L., Poschlod, P., Prinzing, A., Proulx, R., Rammig, A., Reinsch, S., Reu, B., Sack, L.,
915   Salgado-Negret, B., Sardans, J., Shiodera, S., Shipley, B., Siefert, A., Sosinski, E.,
916   Soussana, J.-F., Swaine, E., Swenson, N., Thompson, K., Thornton, P., Waldram,
917   M., Weiher, E., White, M., White, S., Wright, S. J., Yguel, B., Zaehle, S., Zanne, A. E.
918   and Wirth, C (2011) TRY - a global database of plant traits. *Global Change Biology*,
919   **17**, 2905–2935.

920 King, D.A., Davies, S. J., Tan, S., & Noor, N. S. M. (2006) The role of wood density and stem
921   support costs in the growth and mortality of tropical trees. *Journal of Ecology*, **94**,
922   670-680.

923 Kunstler, G., Falster, D., Coomes, D.A., Hui, F., Kooyman, R.M., Laughlin, D.C., Poorter, L.,
924   Vanderwel, M., Vieilledent, G., Wright, S.J., Aiba, M., Baraloto, C., Caspersen, J.,
925   Cornelissen, J.H., Gourlet-Fleury, S., Hanewinkel, M., Herault, B., Kattge, J.,
926   Kurokawa, H., Onoda, Y., Penuelas, J., Poorter, H., Uriarte, M., Richardson, S., Ruiz-
927   Benito, P., Sun, I.F., Stahl, G., Swenson, N.G., Thompson, J., Westerlund, B., Wirth,
928   C., Zavala, M.A., Zeng, H., Zimmerman, J.K., Zimmermann, N.E. & Westoby, M.
929   (2016) Plant functional traits have globally consistent effects on competition. *Nature*,
930   **529**, 204-7.

931 Laanisto, L. & Niinemets, Ü. (2015) Polytolerance to abiotic stresses: how universal is the
932   shade-drought tolerance trade-off in woody species? *Global Ecology &*
933   *Biogeography*, **24**, 571-580.

934 Laliberté, E., Legendre, P., & Shipley, B. (2014) *FD: Measuring functional diversity (FD) from*
935   *multiple traits, and other tools for functional ecology. R package version 1.0-12.*

936 Langan, L., Higgins, S.I. & Scheiter, S. (2017) Climate-biomes, pedo-biomes or pyro-biomes:
937   which world view explains the tropical forest–savanna boundary in South America?
938   *Journal of Biogeography*, **44**, 2319-2330.

3

939 Lausch, A., Bastian, O., Klotz, S., Leitão, P.J., Jung, A., Rocchini, D., Schaepman, M.E.,
940   Skidmore, A.K., Tischendorf, L., & Knapp, S. (2018) Understanding and assessing
941   vegetation health by in situ species and remote-sensing approaches. *Methods in*
942   *Ecology and Evolution*, **9**, 1799-1809.

943 Lavorel, S. & Garnier, E. (2002a) Predicting Changes in Community Composition and
944   Ecosystem Functioning from Plant Traits:

945 Revisiting the Holy Grail. *Functional Ecology*, **16**, 545-556.

946 Lavorel, S. & Garnier, E. (2002b) Predicting changes in community composition and
947   ecosystem functioning from plant traits: revisiting the Holy Grail. *Functional Ecology*,
948   **16**, 545-556.

949 Lavorel, S., Diaz, S., Cornelissen, J.H.C., Garnier, E., Harrison, S.P., McIntyre, S., Pausas,
950   J.G., Perez-Harguinedeguy, Roumet, C. & Urcelay, C. (2007) Plant Functional
951   Types: Are We Getting Any Closer to the Holy Grail? *Terrestrial Ecosystems in a*
952   *Changing World* (ed. by C. Jp, P. D and P. Lf), pp. 149-160. Springer, Berlin,
953   Heidelberg, New York.

954 Lefsky, M.A., M. Keller, Y. Pang, P.B. De Camargo, and M.O. Hunter (2007) Revised
955   method for forest canopy height estimation from Geoscience Laser Altimeter System
956   waveforms. *Journal of Applied Remote Sensing*, **1**, 013537-013518.

957 Liang, J., Crowther, T.W., Picard, N., Wiser, S., Zhou, M., Alberti, G., Schulze, E.D.,
958   McGuire, A.D., Bozzato, F., Pretzsch, H., de-Miguel, S., Paquette, A., Herault, B.,
959   Scherer-Lorenzen, M., Barrett, C.B., Glick, H.B., Hengeveld, G.M., Nabuurs, G.J.,
960   Pfautsch, S., Viana, H., Vibrans, A.C., Ammer, C., Schall, P., Verbyla, D.,
961   Tchebakova, N., Fischer, M., Watson, J.V., Chen, H.Y., Lei, X., Schelhaas, M.J., Lu,
962   H., Gianelle, D., Parfenova, E.I., Salas, C., Lee, E., Lee, B., Kim, H.S., Bruelheide,
963   H., Coomes, D.A., Piotto, D., Sunderland, T., Schmid, B., Gourlet-Fleury, S., Sonke,
964   B., Tavani, R., Zhu, J., Brandl, S., Vayreda, J., Kitahara, F., Searle, E.B., Neldner,
965   V.J., Ngugi, M.R., Baraloto, C., Frizzera, L., Balazy, R., Oleksyn, J., Zawila-
966   Niedzwiecki, T., Bouriaud, O., Bussotti, F., Finer, L., Jaroszewicz, B., Jucker, T.,
967   Valladares, F., Jagodzinski, A.M., Peri, P.L., Gonmadje, C., Marthy, W., O'Brien, T.,
968   Martin, E.H., Marshall, A.R., Rovero, F., Bitariho, R., Niklaus, P.A., Alvarez-Loayza,
969   P., Chamuya, N., Valencia, R., Mortier, F., Wortel, V., Engone-Obiang, N.L., Ferreira,
970   L.V., Odeke, D.E., Vasquez, R.M., Lewis, S.L. & Reich, P.B. (2016) Positive
971   biodiversity-productivity relationship predominant in global forests. *Science*, **354**

972 Liebergesell, M., Reu, B., Stahl, U., Freiberg, M., Welk, E., Kattge, J., Cornelissen, J.H.,
973   Penuelas, J. & Wirth, C. (2016) Functional Resilience against Climate-Driven
974   Extinctions - Comparing the Functional Diversity of European and North American
975   Tree Floras. *PLoS One*, **11**, e0148607.

976 Madrigal-Gonzalez, J., Ruiz-Benito, P., Ratcliffe, S., Calatayud, J., Kandler, G., Lehtonen,
977   A., Dahlgren, J., Wirth, C. & Zavala, M.A. (2016) Complementarity effects on tree
978   growth are contingent on tree size and climatic conditions across Europe. *Scientific*
979   *Reports*, **6**, 10.

980 Mason, N.W.H. & de Bello, F. (2013) Functional diversity: a tool for answering challenging
981   ecological questions. *Journal of Vegetation Science*, **24**, 777-780.

982 Mason, N.W.H., Mouillot, D., Lee, W.G. & Wilson, J.B. (2005) Functional richness, functional
983   evenness and functional divergence: the primary components of functional diversity.
984   *Oikos*, **111**, 112-118.

985 Mason, N.W.H., de Bello, F., Mouillot, D., Pavoine, S. & Dray, S. (2013) A guide for using
986   functional diversity indices to reveal changes in assembly processes along ecological
987   gradients. *Journal of Vegetation Science*, **24**, 794-806.

988 Mitchell, T.D. (2002) A comprehensive set of climate scenarios for Europe. *in prep.*,

989 Mori, A.S., Lertzman, K.P. & Gustafsson, L. (2017) Biodiversity and ecosystem services in
990   forest ecosystems: a research agenda for applied forest ecology. *Journal of Applied*
991   *Ecology*, **54**, 12-27.

992 Mouillot, D., Graham, N.A.J., Villeger, S., Mason, N.W.H. & Bellwood, D.R. (2013) A
993   functional approach reveals community responses to disturbances. *Trends in*
994   *Ecology & Evolution*, **28**, 167-177.

995 Nachtergaele, F., van Velthuizen, H., Verelst, L., Batjes, N., Dijkshoorn, K., van Engelen, V.,
996   Fischer, G., Jones, A., & Montanarella, L., and Petri, M. (2009) Harmonized world
997   soil database, Food and Agriculture Organization of the United Nations. In: (ed. Fao),
998   Rome.

999 Naeem, S., Duffy, J.E. & Zavaleta, E.S. (2012) The functions of biological diversity in an Age
1000   of Extinction. *Science*, **336**, 1401-1406.

1001 Naveh, Z. (1990) Fire in the Mediterranean - a landscape ecological perspective. *Fire in*
1002   *ecosystem dynamics: Mediterranean and Northern perspectives* (ed. by J.G.
1003   Goldammer and M.J. Jenkins). SPB Academic Publ., The Hague.

1004 Niinemets, Ü. & Valladares, F. (2006) Tolerance to shade, drought and waterlogging in the
1005   temperate dendroflora of the Northern hemisphere: tradeoffs, phylogenetic signal and
1006   implications for niche differentiation. *Ecological Monographs*, **76**, 521-547.

1007 Pakeman, R.J. (2011) Functional diversity indices reveal the impacts of land use
1008   intensification on plantcommunity assembly. *Journal of Ecology*, **99**, 1143-1151.

1009 Papale, D., Reichstein, M., Aubinet, M., Canfora, E., Bernhofer, C., Kutsch, W. & Yakir, D.
1010   (2006) Towards a standardized processing of Net Ecosystem Exchange measured
1011   with eddy covariance technique: algorithms and uncertainty estimation.
1012   *Biogeosciences*, **3**, 571-583.

1013 Paul-Limoges, E., Damm, A., Hueni, A., Liebisch, F., Eugster, W., Schaepman, M.E., &
1014   Buchmann, N. (2018) Effect of environmental conditions on sun-induced
1015   fluorescence in a mixed forest and a cropland. *Remote Sensing of Environment*, **219**,
1016   310-323.

1017 Prentice, I., Bondeau, A., Cramer, W., Harrison, S., Hickler, T., Lucht, W., Sitch, S., Smith,
1018   B. & Sykes, M. (2007) Dynamic global vegetation modelling: quantifying terrestrial
1019   ecosystem responses to large-scale environmental change. . *Terrestrial Ecosystems*
1020   *in a Changing World* (ed. by C. Jp, P. D and P. Lf). Springer, Berlin, Heidelberg, New
1021   York.

1022 Ratcliffe, S., Liebergesell, M., Ruiz-Benito, P., Madrigal González, J., Muñoz Castañeda,
1023   J.M., Kändler, G., Lehtonen, A., Dahlgren, J., Kattge, J., Peñuelas, J., Zavala, M.A. &
1024   Wirth, C. (2016) Modes of functional biodiversity control on tree productivity across
1025   the European continent. *Global Ecology and Biogeography*, **25**, 251-262.

1026 Ratcliffe, S., Wirth, C., Jucker, T., van der Plas, F., Scherer-Lorenzen, M., Verheyen, K.,
1027   Allan, E., Benavides, R., Bruelheide, H., Ohse, B., Paquette, A., Ampoorter, E.,
1028   Bastias, C.C., Bauhus, J., Bonal, D., Bouriaud, O., Bussotti, F., Carnol, M.,
1029   Castagneyrol, B., Checko, E., Dawud, S.M., De Wandeler, H., Domisch, T., Finer, L.,
1030   Fischer, M., Fotelli, M., Gessler, A., Granier, A., Grossiord, C., Guyot, V., Haase, J.,
1031   Hattenschwiler, S., Jactel, H., Jaroszewicz, B., Joly, F.X., Kambach, S., Kolb, S.,
1032   Koricheva, J., Liebersgesell, M., Milligan, H., Muller, S., Muys, B., Nguyen, D., Nock,
1033   C., Pollastrini, M., Purschke, O., Radoglou, K., Raulund-Rasmussen, K., Roger, F.,
1034   Ruiz-Benito, P., Seidl, R., Selvi, F., Seiferling, I., Stenlid, J., Valladares, F., Vesterdal,
1035   L. & Baeten, L. (2017) Biodiversity and ecosystem functioning relations in European
1036   forests depend on environmental context. *Ecology Letters*, **20**, 1414-1426.

1037 Reich, P.B. (2014) The world-wide 'fast–slow' plant economics spectrum: a traits manifesto.
1038   *Journal of Ecology*, **102**, 275-301.

1039 Reichstein, M., Falge, E., Baldocchi, D., Papale, D., Aubinet, M., Berbigier, P. & Grünwald,
1040   T. (2005) On the separation of net ecosystem exchange into assimilation and
1041   ecosystem respiration: review and improved algorithm. *Global Change Biology*, **11**,
1042   1424-1439.

1043 Ruiz-Benito, P., Ratcliffe, S., Jump, A.S., Gomez-Aparicio, L., Madrigal-Gonzalez, J., Wirth,
1044   C., Kandler, G., Lehtonen, A., Dahlgren, J., Kattge, J. & Zavala, M.A. (2017)
1045   Functional diversity underlies demographic responses to environmental variation in
1046   European forests. *Global Ecology and Biogeography*, **26**, 128-141.

1047 Running, S. (2015) MODIS/TERRA Gross Primary Productivity 8-Day L4 Global 500 m SIN
1048   Grid V006. In: (ed. U.E.R.O.a.S.E.C. Nasa Eosdis Land Processes Daac), Sioux
1049   Falls, South Dakota (Https://Lpdaac.Usgs.Gov).

1050 Sakschewski, B., von Bloh, W., Boit, A., Rammig, A., Kattge, J., Poorter, L., Penuelas, J. &
1051   Thonicke, K. (2015) Leaf and stem economics spectra drive diversity of functional
1052   plant traits in a dynamic global vegetation model. *Global Change Biology*, **21**, 2711-
1053   2725.

1054 Sandel, B., Gutierrez, A.G., Reich, P.B., Schrodt, F., Dickie, J. & Kattge, J. (2015) Estimating
1055   the missing species bias in plant trait measurements. *Journal of Vegetation Science*,
1056   **26**, 828-838.

1057 Schaphoff, S., Forkel, M., Müller, C., Knauer, J., von Bloh, W., Gerten, D., Jägermeyr, J.,
1058   Lucht, W., Rammig, A., Thonicke, K. & Waha, K. (2018a) LPJmL4 – a dynamic global
1059   vegetation model with managed land – Part 2: Model evaluation. *Geoscientific Model
1060   Development*, **11**, 1377-1403.

1061 Schaphoff, S., von Bloh, W., Rammig, A., Thonicke, K., Biemans, H., Forkel, M., Gerten, D.,
1062   Heinke, J., Jägermeyr, J., Knauer, J., Langerwisch, F., Lucht, W., Müller, C., Rolinski,
1063   S. & Waha, K. (2018b) LPJmL4 – a dynamic global vegetation model with managed
1064   land – Part 1: Model description. *Geoscientific Model Development*, **11**, 1343-1375.

1065 Schneider, F.D., Morsdorf, F., Schmid, B., Petchey, O.L., Hueni, A., Schimel, D.S. &
1066   Schaepman, M.E. (2017) Mapping functional diversity from remotely sensed
1067   morphological and physiological forest traits. *Nat Commun*, **8**, 1441.

1068 Schneider, U., Becker, A., Finger, P., Meyer-Christoffer, A., Rudolf, B. & Ziese, M. (2011)
1069   GPCC Full Data Reanalysis Version 6.0 at 0.5°: Monthly Land-Surface Precipitation
1070   from Rain-Gauges built on GTS-based and Historic Data.

1071 Šímová, I., Violle, C., Svenning, J.-C., Kattge, J., Engemann, K., Sandel, B., Peet, R.K.,
1072   Wiser, S.K., Blonder, B., McGill, B.J., Boyle, B., Morueta-Holme, N., Kraft, N.J.B.,
1073   van Bodegom, P.M., Gutiérrez, A.G., Bahn, M., Ozinga, W.A., Tószögyová, A. &
1074   Enquist, B.J. (2018) Spatial patterns and climate relationships of major plant traits in
1075   the New World differ between woody and herbaceous species. *Journal of
1076   Biogeography*, **45**, 895-916.

1077 Sitch, S., Smith, B., Prentice, I.C., Arneth, A., Bondeau, A., Cramer, W., Kaplan, J.O., Levis,
1078   S., Lucht, W., Sykes, M.T., Thonicke, K. & Venevsky, S. (2003) Evaluation of
1079   ecosystem dynamics, plant geography and terrestrial carbon cycling in the LPJ
1080   Dynamic Global Vegetation Model. *Global Change Biology*, **9**, 161-185.

1081 Sitch, S., Huntingford, C., Gedney, N., Levy, P.E., Lomas, M., Piao, S.L., Betts, R.A., Ciais,
1082   P., Cox, P.M., Friedlingstein, P., Jones, C.D., Prentice, I.C. & Woodward, F.I. (2008)
1083   Evaluation of the terrestrial carbon cycle, future plant geography and climate-carbon
1084   cycle feedbacks using five Dynamic Global Vegetation Models (DGVMs). *Global
1085   Change Biology*, **14**, 2015-2039.

1086   Thonicke, K., Venevsky, S., Sitch, S. & Cramer, W. (2001) The role of fire disturbance for
1087   global vegetation dynamics: coupling fire into a Dynamic Global Vegetation Model.
1088   *Global Ecology and Biogeography*, **10**, 661-677.

1089   Thurner, M., Beer, C., Santoro, M., Carvalhais, N., Wutzler, T., Schepaschenko, D., ... &
1090   Schmullius, C. (2014) Carbon stock and density of northern boreal and temperate
1091   forests. *Global Ecology and Biogeography*, **23**, 297-310.

1092   Tinner, W., Hubschmid, P., Wehrli, M., Ammann, B., & Conedera, M. (1999) Long-term
1093   forest fire ecology and dynamics in southern Switzerland. *Journal of Ecology*, **87**,
1094   273-289.

1095   Van Bodegom, P.M., Douma, J.C., Witte, J.P.M., Ordoñez, J.C., Bartholomeus, R.P. &
1096   Aerts, R. (2012) Going beyond limitations of plant functional types when predicting
1097   global ecosystem-atmosphere fluxes: exploring the merits of traits-based
1098   approaches. *Global Ecology and Biogeography*, **21**, 625-636.

1099   Villeger, S., Mason, N.W.H. & Mouillot, D. (2008) New multidimensional functional diversity
1100   indices for a multifaceted framework in functional ecology. *Ecology*, **89**, 2290-2301.

1101   Weedon, G.P., Balsamo, G., Bellouin, N., Gomes, S., Best, M. J., & Viterbo, P. (2014) The
1102   WFDEI meteorological forcing data set: WATCH Forcing Data methodology applied
1103   to ERA-Interim reanalysis data *Water Resources Research*, **50**, 7505–7514.

1104   Weedon, G.P., Gomes, S., Viterbo, P., Shuttleworth, W. J., Blyth, E., Österle, H., … Best, M.
1105   (2011) Creation of the WATCH Forcing Data and Its Use to Assess Global and
1106   Regional Reference Crop Evaporation over Land during the Twentieth Century.
1107   *Journal of Hydrometeorology*, **12** 823–848.

1108   Wright, I.J., Ning Dong, Maire, V., Prentice, I.C., Westoby, M., Díaz, S., Gallagher, R.V.,
1109   Jacobs, B.F., Kooyman, R., Law, E.A., Leishman, M.R., Niinemets, Ü., Reich, P.B.,
1110   Sack, L., Villar, R., Wang, H. & Wilf, P. (2017) Global climatic drivers of leaf size.
1111   *Science*, **357**, 917-921.

1112   Wright, I.J., Peter B. Reich, Mark Westoby, David D. Ackerly, Zdravko Baruch, Frans
1113   Bongers, Jeannine Cavender-Bares, Terry Chapin, Johannes H. C. Cornelissen,
1114   Matthias Diemer, Jaume Flexas, Eric Garnier, Philip K. Groom, Javier Gulias, Kouki
1115   Hikosaka, Byron B. Lamont, Tali Lee, William Lee, Christopher Lusk, Jeremy J.
1116   Midgley, Marie-Laure Navas, Ülo Niinemets, Jacek Oleksyn, Noriyuki Osada, Hendrik
1117   Poorter, Pieter Poot, Lynda Prior, Vladimir I. Pyankov, Catherine Roumet, Sean C.
1118   Thomas, Mark G. Tjoelker, Veneklaas, E.J. & Villar, R. (2004) The worldwide leaf
1119   economics spectrum. *Nature* **428**, 821-827.

1120   Zhang, T., Niinemets, U., Sheffield, J. & Lichstein, J.W. (2018) Shifts in tree functional
1121   composition amplify the response of forest biomass to climate. *Nature*, **556**, 99-102.

1122